高強度超冷中性子源による
中性子電気双極子モーメント探索

川崎真介

KEK

Contents

- Electric-Dipole Moment
- Ultra-Cold Neutron (UCN)
  - 特徴
  - UCNを用いた物理
  - UCN生成方法
- nEDM measurement
  - nEDM experiment at ILL/PSI
  - TUCAN
    - UCN源開発
    - 測定器開発　(今日は少しだけ)
    - 計画
- まとめ

T̲RIUMF U̲ltra-C̲old A̲dvanced N̲eutron

日本ーカナダの国際共同実験

B. Bell[5,8], C. Bidinosti[3], C. Davis[5], B. Franke[2,5], M. Gericke[4], P. Giampa[5], S. Hansen-Romu[3,4], K. Hatanaka[6], T. Hayamizu[11], T. Higuchi[6], G. Ichikawa[1], S. Imajo[6], B. Jamieson[3], S. Kawasaki[1], M. Kitaguchi[10], W. Klassen[3,4], A. Konaka[5], E. Korkmaz[7], M. Lang[3,4], M. Lavvaf[3], L. Lee[5], T. Lindner[3,5], K. Madison[2], Y. Makida[1], J. Mammei[4], R. Mammei[3,5], C. Marshall[5], J. W. Martin[3], R. Matsumiya[5], M. McCrea[3], E. MIller[2], K. Mishima[1],T. Momose[2], T. Okamura[1], O. H. Jin[6], R. Picker[5,9], W. D. Ramsey[5], LW. Schreyer[5], H. SHimizu[10], S. Sidhu[9], I. Tanihata[6], W. T. H. van Oers[4,5], and Y. Watanabe[1]–

[1]KEK, [2]The University of British Columbia
[3]The University of Winnipeg, [4]The University of Manitoba
[5]TRIUMF, [6]RCNP, [7]The University of Northern BC
[8]McGill University, [9]Simon Fraser University
[10]Nagoya University, [11]Riken

TUCANの目標

- **中性子電気双極子モーメントを 10^{-27} ecmの精度で測定する**
- **世界最大強度の超冷中性子源を建設する**

Electric Dipole Moment (EDM)

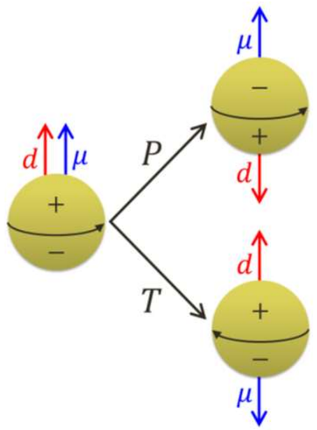

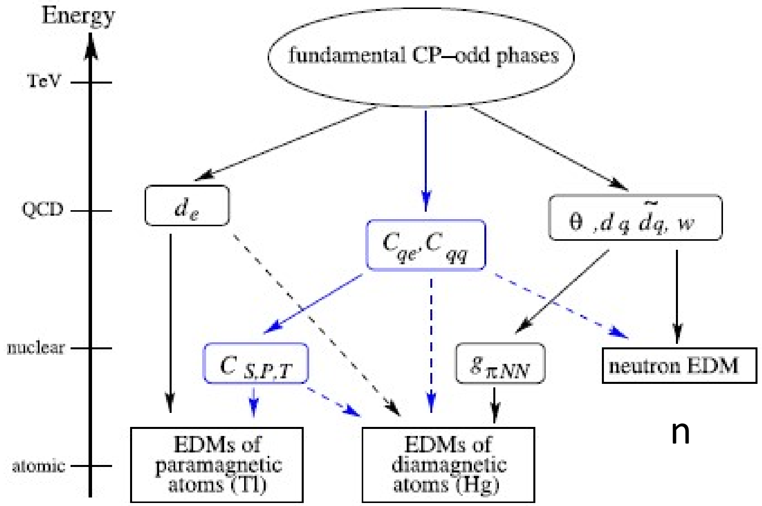

n

Tl, Fr, Cs....

^{199}Hg, ^{129}Xe, Rn, Ra...

Maxim Pospelov and Adam Ritz,
Annals of Physics 318 (2005) 119–169

- Electric dipole moment (EDM)
  - Vector derived from charge distribution

$$\vec{d} = d\frac{\vec{s}}{|\vec{s}|}$$

unit e cm

	P	T
spin	Even	Odd
EDM	Odd	Even

d≠0 → T Violation

Assume CPT conservation

→ CP Violation

new source of CP violation?

EDM search in various kind of system is important to understand nature of physics

EDMの大きさ

- 例えば中性子EDMの場合

$$|d_{\mathrm{n}}| < 1.8 \times 10^{-26}\ \mathrm{ecm}$$

Phys. Rev. Lett 124,081803 (2020)

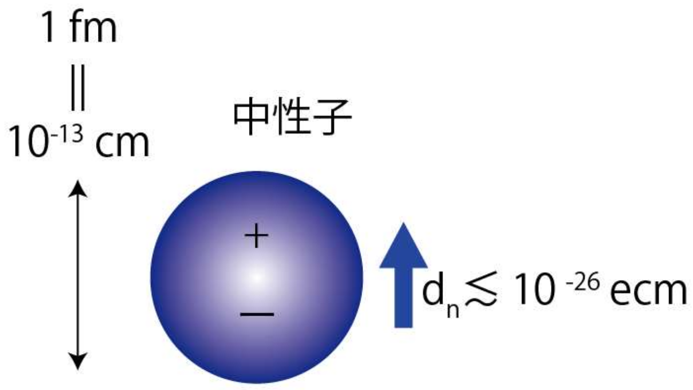

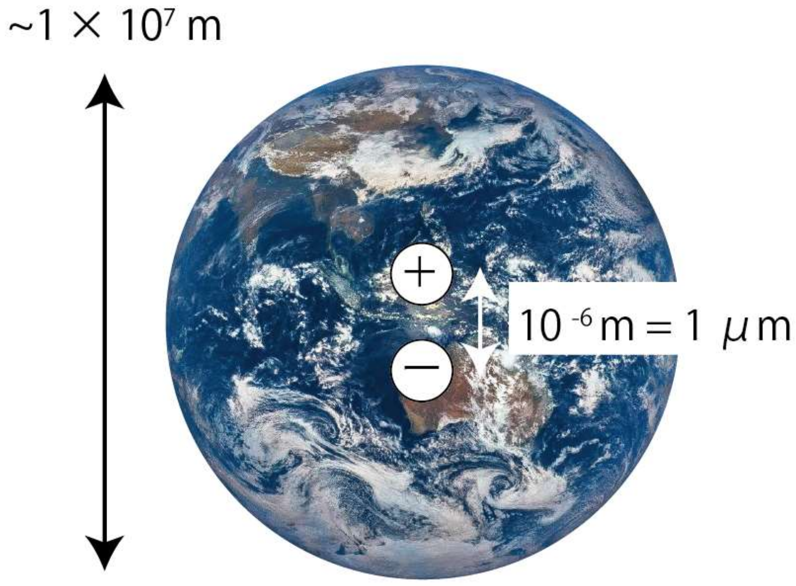

地球の大きさの中から1μm離れた素電荷のを見つけるのと同じスケール感

EDMの測定方法

$$\boxed{H = -\vec{\mu}\cdot\vec{B} + \vec{d}\cdot\vec{E}}$$

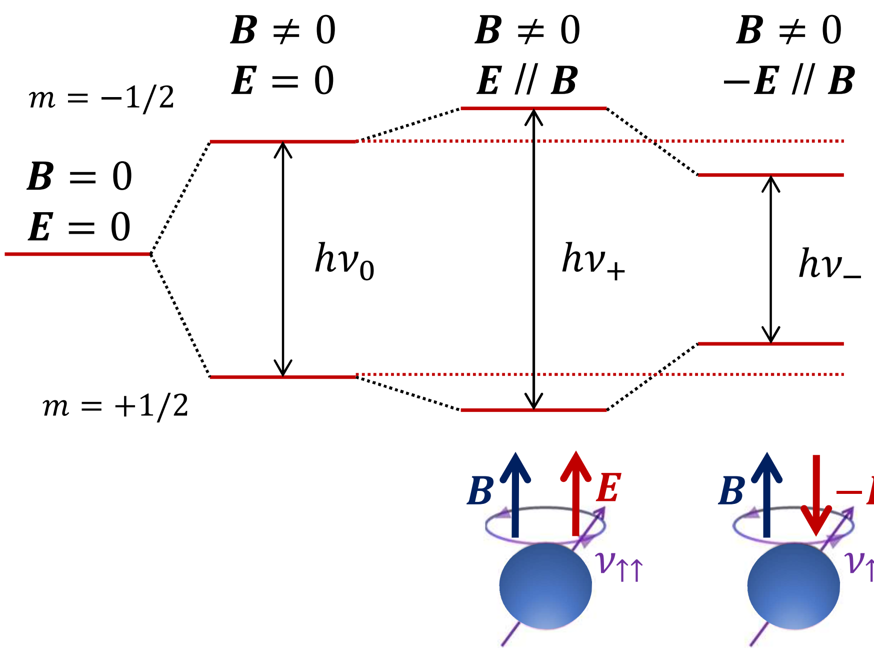

$$\nu_{\uparrow\uparrow} = \frac{2\mu B + 2dE}{h} \qquad \nu_{\uparrow\downarrow} = \frac{2\mu B - 2dE}{h}$$

figure from K. Asahi

(理想的)
電磁場中のスピン歳差運動周期の差を測定

$$\Delta\nu = \nu_{\uparrow\uparrow} - \nu_{\uparrow\downarrow} = \frac{4dE}{h}$$

d = 10^{-26} ecm, E = 10 kV/cmの時

Δν＝1 μHz

Cf. 中性子のラーモア周波数(ν_0)
30 Hz/μT

ラムゼー共鳴法

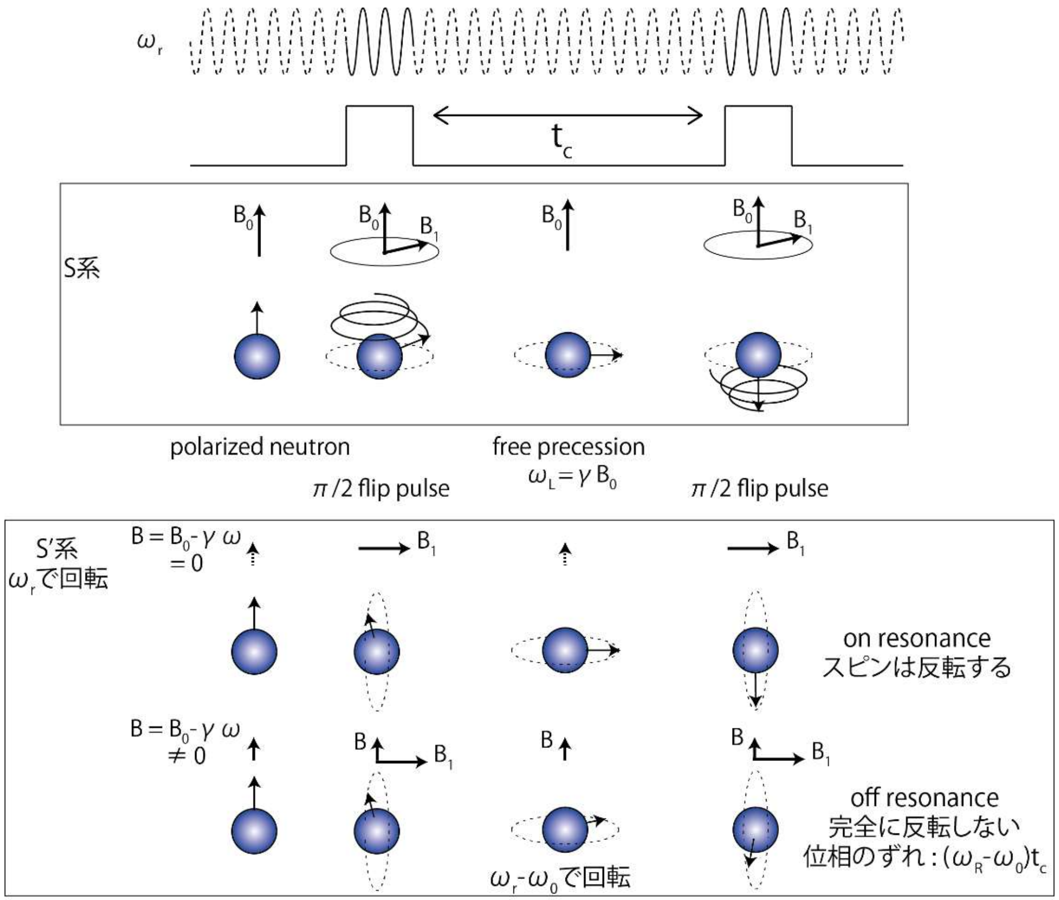

位相のずれがt_c間蓄積される

ラムゼー共鳴法

ある間隔をあけて粒子とコヒーレントな電磁場を2度相互作用させたときに生じる共鳴現象。時間間隔が大きい程共鳴の線幅は電磁場間の時間間隔に反比例して小さくなる

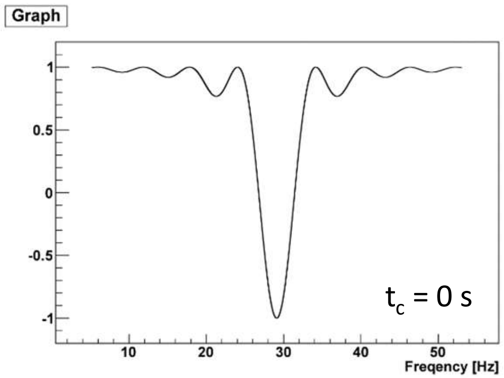

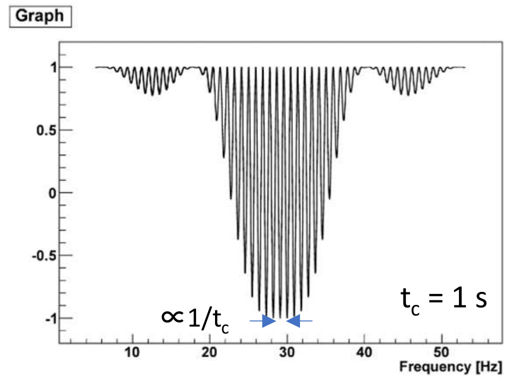

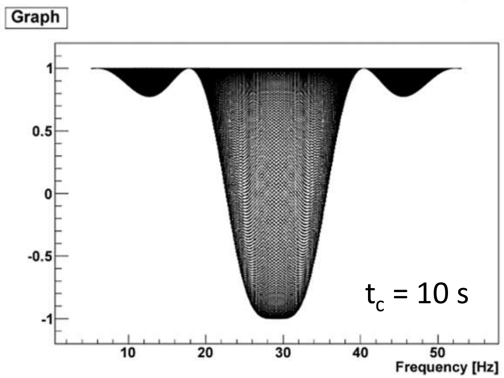

B_0 = 1 μT

B_1 = 0.1 μT の時

細かいフリンジの周期はt_cに比例して細かくなり、周波数決定精度が向上する

実際は

この項が消え切らない

$$\Delta\nu = \nu_{\uparrow\uparrow} - \nu_{\uparrow\downarrow} = \frac{2\mu\boxed{(\mathrm{B}_{\uparrow\uparrow} - \mathrm{B}_{\uparrow\downarrow}})}{h} + \frac{4d\boxed{E}}{h}$$

高精度のEDM測定には

・Bの精密制御

E = 10 kV/cmでd = 10^{-26} ecmを測定する場合

$$\Delta B = (\mathrm{B}_{\uparrow\uparrow} - \mathrm{B}_{\uparrow\downarrow}) \ll \frac{dE}{\mu} \sim 10\ \mathrm{fT}$$

磁場を精密に制御するために

- 磁気シールド
- 磁束計
  - SQUID, Cs, Rb
  - Co-magnetometer (^{199}Hg, ^{3}He)

の開発が重要

・大きなE

・高電場

・分子、結晶内の有効電場

History of EDM search

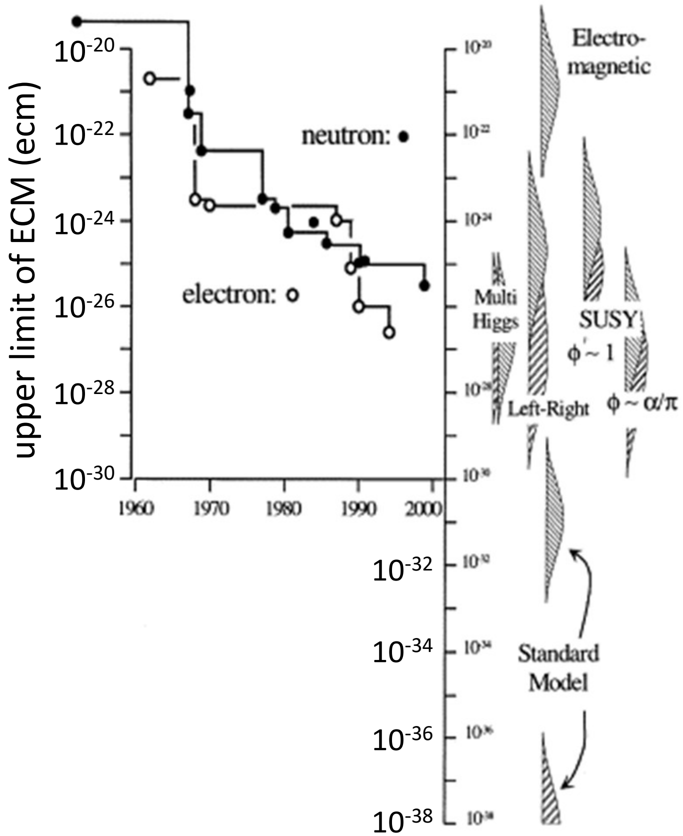

Pendlebury and Hinds, NIM A 440 (00) 471

upper limit

neutron EDM

$|d_n| < 1.8 \times 10^{-26}$ ecm UCN — C. Abel et al. Phys. Rev. Lett. 124, 081803 (2020)

electron EDM

$|d_e| < 1.6 \times 10^{-27}$ ecm Cs

$|d_e| < 1.6 \times 10^{-27}$ ecm Tl — B.C. Regan et al, PRL 88, 071805 (2002)

$|d_e| < 10.5 \times 10^{-28}$ ecm YbF — J. J. Hudson et al, Nature 473, 493 (2011)

$|d_e| < 8.7 \times 10^{-29}$ ecm ThO — The ACME Collaboration et al, Science, 343, 269 (2014)

atomic EDM

$|d_{Hg}| < 7.4 \times 10^{-30}$ ecm ^{199}Hg — B. Garner et al., PRL 116 161601 (2016)

$|d_{Xe}| < 1.5 \times 10^{-27}$ ecm ^{129}Xe — F. Allmendinger et al, Phys. Rev. A 100, 022505 (2019)

muon EDM

$|d_\mu| < 1.8 \times 10^{-19}$ ecm — G. W. Bennett et al, Phys. Rev. D 80, 052008 (2009)

Standard model prediction

neutron : $10^{-30} - 10^{-32}$ ecm

electron : $10^{-37} - 10^{-40}$ ecm

much smaller than current experimental sensitivity

good probe of testing new physics

中性子EDM

中性子EDM探索の歴史

nEDM測定の歴史

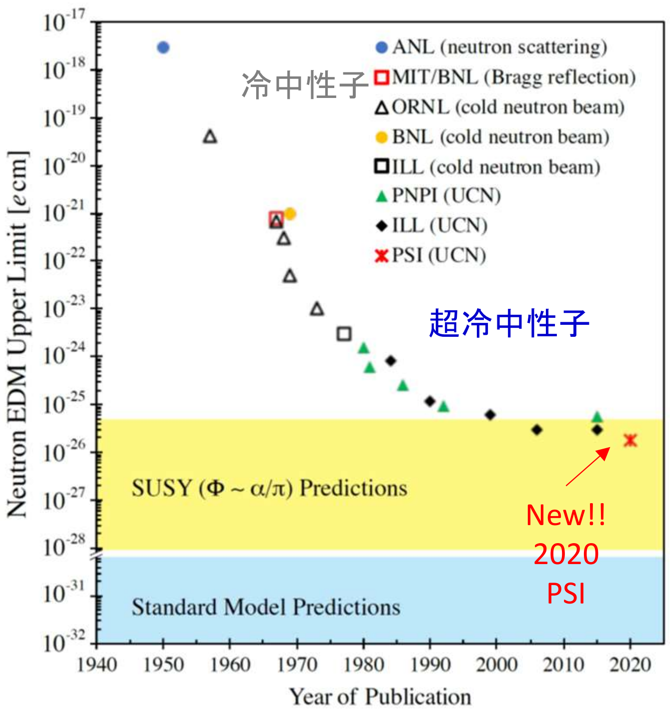

初期は冷中性子ビームを用いた測定。
1980年頃より超冷中性子を用いた蓄積実験が行われるようになり感度が向上。

neutron mirror

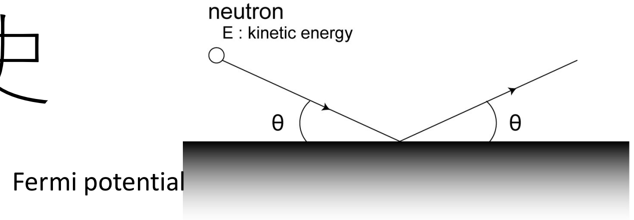

鉛直方向の運動エネルギーがフェルミポテンシャルより小さい場合は中性子は物質表面で反射する

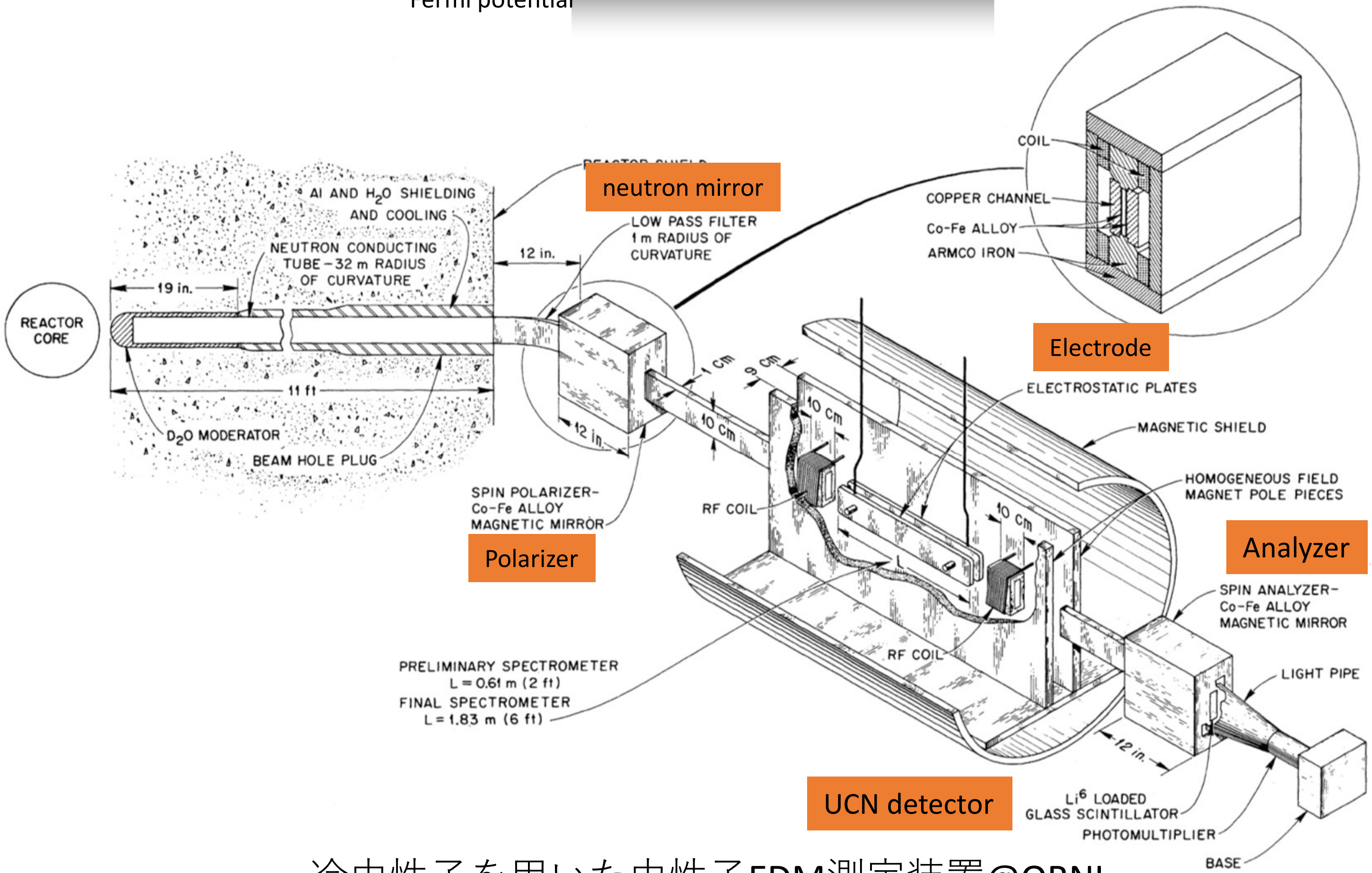

冷中性子を用いた中性子EDM測定装置@ORNL
Phys. Rev. Lett. **14**, 381 (1967)

Various neutrons

Fast

Name	Energy	Wavelength	Velocity	Temperature	Application
Fast neutron	>500 keV	40 fm	10^7 m/s	6×10^9 K	Nuclear physics Astro physics
Epi-themral neutron	10 eV	0.1 Å	44,000 m/s	1×10^5 K	Resonance capture
Thermal neutron	25 meV	1.8 Å	2200 m/s	300 K	Neutron scattering
Cold neutron	2 meV	6 Å	600 m/s	23 K	Neutron scattering for condensed matter (nm)
Very cold neutron	50 μeV	40Å	100 m/s	0.6 K	Neutron interferometer
Ultra-cold netruon UCN	**<300 neV**	**500Å**	**8 m/s**	**3 mK**	**nEDM etc.**

Slow

Slide by K. Mishima

超冷中性子　Ultra Cold Neutron (UCN)

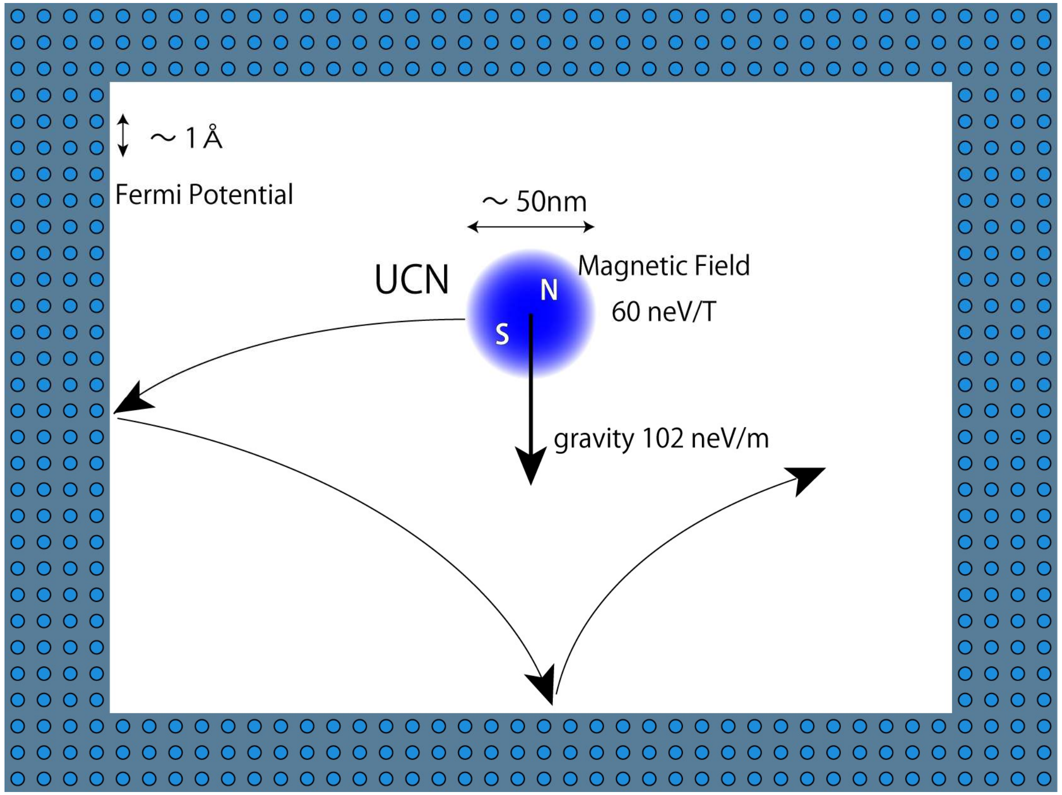

物質、重力、磁場ポテンシャルによるに閉じ込め

長時間（～百秒）の観測が可能

超冷中性子

エネルギー ～ 100 neV
速度 ～ 5 m/s
波長 ～ 50 nm

中性子の受ける力

- 強い相互作用
  フェルミポテンシャル 335 neV (^{58}Ni)
  原子間距離に比べUCNの波長が長いため、個々の原子核のポテンシャルの平均を感じる
- 弱い相互作用
  β-decay　$n \rightarrow p + e + \nu_e$
- 重力場　100 neV/m
- 磁場　60 neV/T

→さまざまな基礎物理実験に用いられる
nEDM、重力、寿命、 …

Physics using UCN

τ_n = (877.7 ± 0.7$_{stat}$ +0.4/-0.2 $_{sys}$) s.

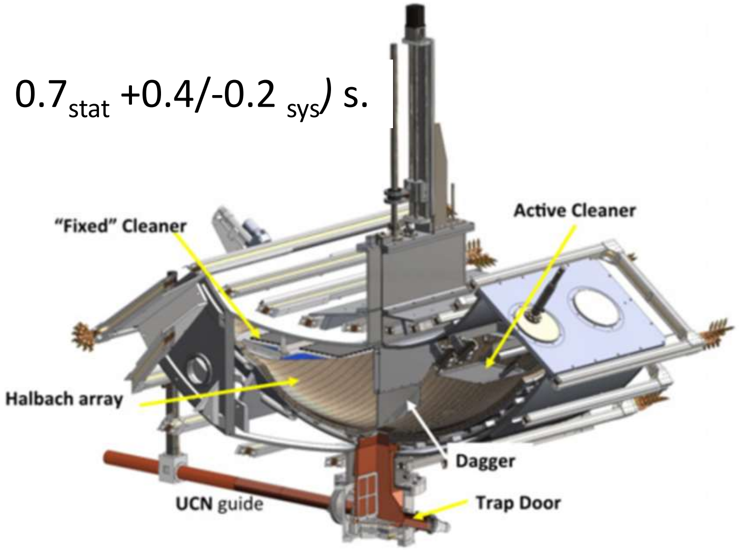

setup of UCNτ experiment (LANL)
magneto-gravity trap
容器にUCNが触れない

- neutron life time measurement
- gravity experiment
- nEDM search

and so on,

High intensity UCN source is necessary

neutron lifetime measurement

MAMBO experiment

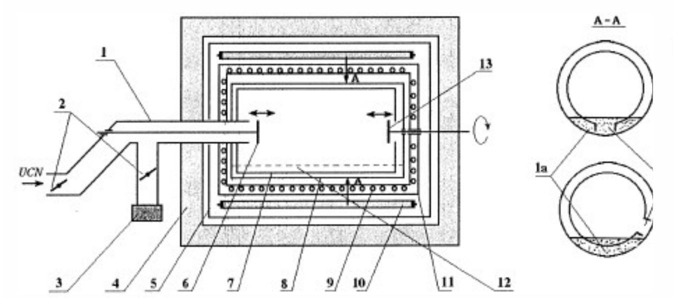

S. Arzumanov et al., Phys. Lett B 483, 15 (2000)
A.P. Serebrov et al., Phys. Lett. B 605, 72 (2005)
A. Pichlmaier et al., Phys. Lett. B,693:221-226 (2010)

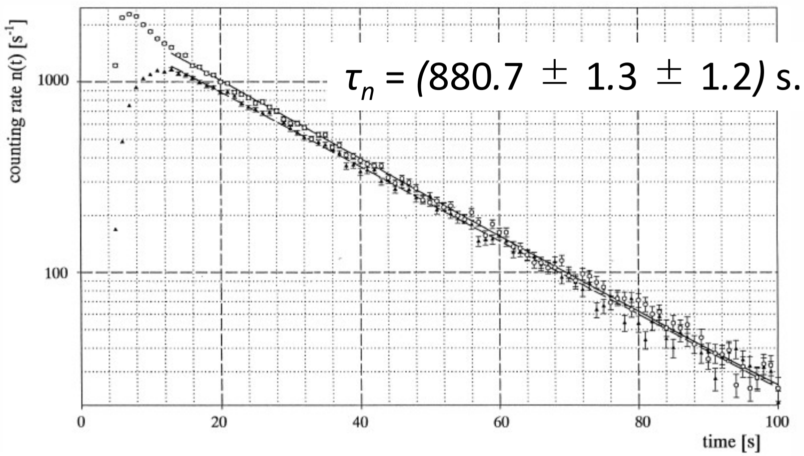

容器表面での散乱(up-scattering)が大きな系統誤差

Gravity experiment

- **Gravity**

potential well

$$V(z)=\begin{cases} mgz & (z\geq 0) \\ \infty & (z<0)\end{cases}$$

Schrödinger equation

$$\left(-\frac{\hbar^2}{2m}\frac{d^2}{dz^2}+\mathrm{V}(z)\right)\psi(\mathrm{z})=\mathrm{E}\,\psi(z)$$

$$\psi(z)=A\,\varphi(z)$$

$$\varphi(z):\text{Airy function}$$

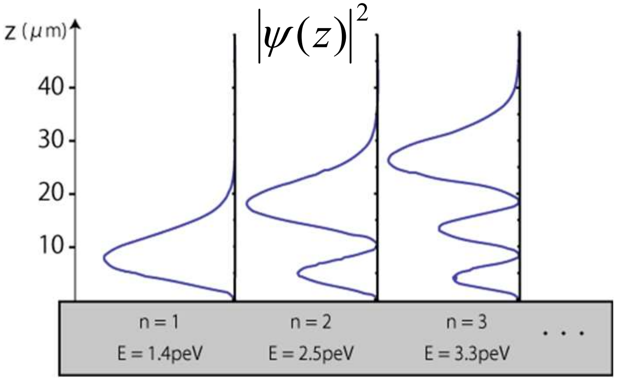

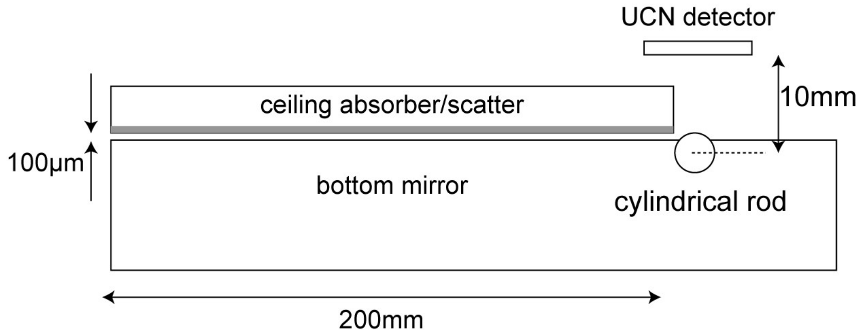

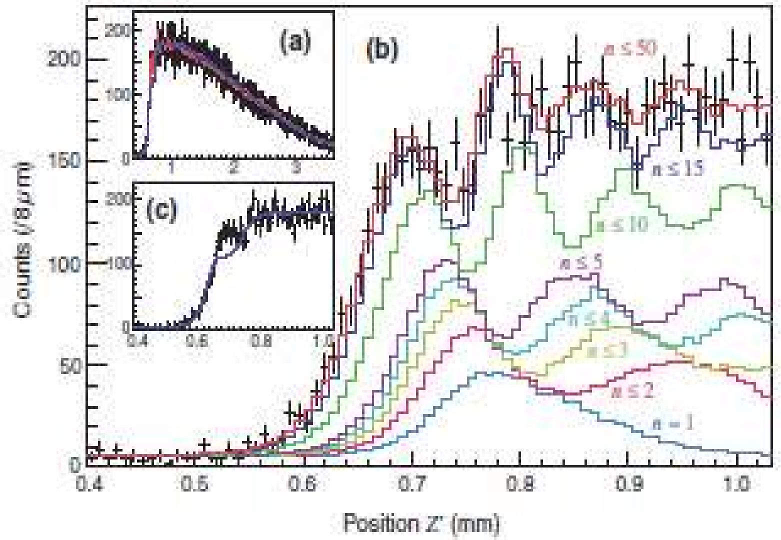

Ichikawa et al., PRL 112, 071101 (2014)

Q-Bounce

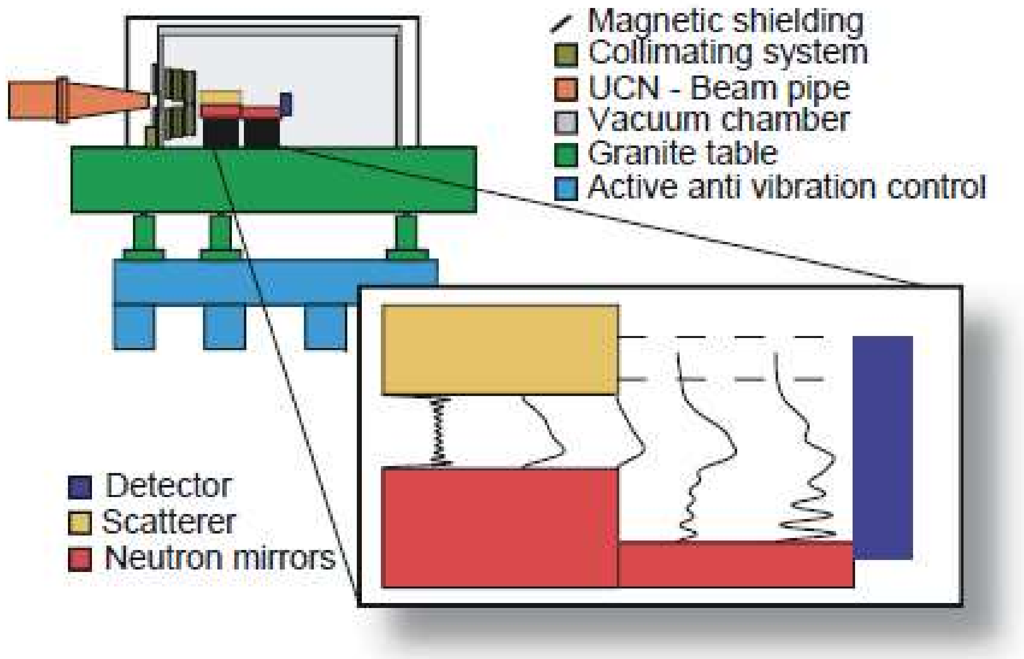

T. Jenke et al. NIM A 611 (2009) 318–321

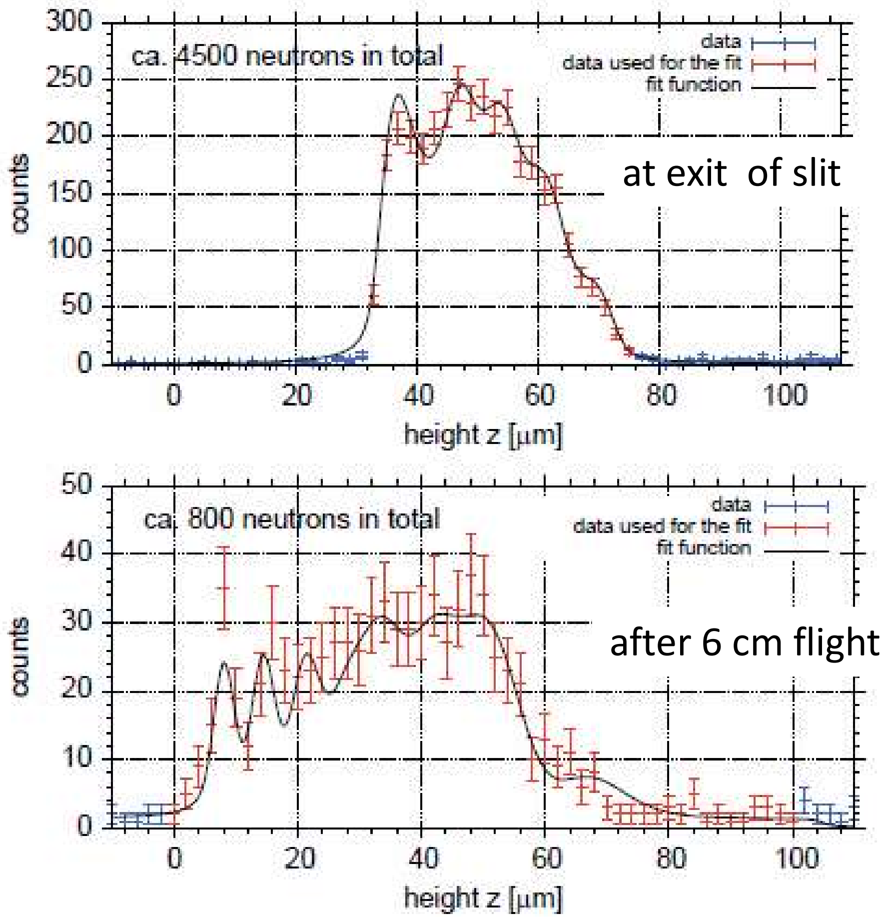

Fig. 3. Simultaneous fit of the square of the Schrödinger wave function to the data shown in the upper and lower figure. Upper figure: preparation of the wave function directly at the step ($x = 0$ cm). Lower figure: measurement at a distance $x = 6$ cm after the same step, quantum prediction after falling and rebouncing.

Measurement of time evolution of quantum state

- UCN fall down at the exit of the slit
- sudden change of boundary condition
- settle new state after certain time evolution

How to produce UCN? (1)
neutron production and thermalization

- Neutron source
  - Reactor
    - JRR3、 ILL(grenoble) etc.
    - Fission of ^{235}U or ^{239}Pu
  - Accelerator (Spallation)
    - J-PARC MLF, SNS, PSI, TRIUMF, LANL etc.
    - spallation reaction induced by proton beam

  produced neutron energy ～ MeV

- Neutron moderation
  - like billiard
  - criteria for a good moderator
    - large scattering cross section
    - U ～ 1u
    - large density　(liquid, solid　≫　gas)
    - small absorb cross section

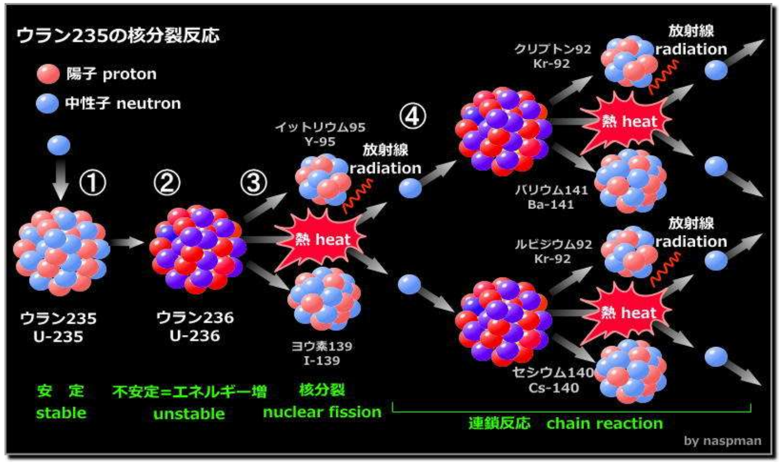

spallation

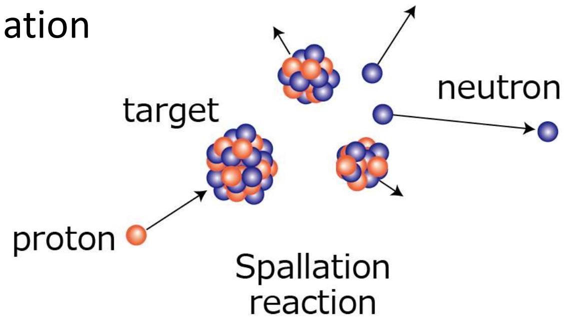

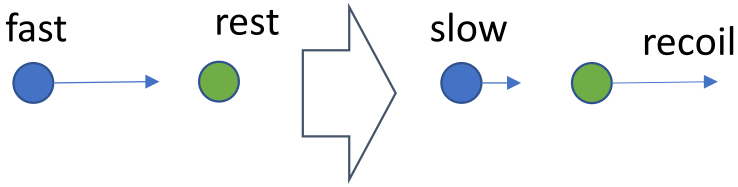

Neutron moderator

- Thermal neutron (300K)
  - light water: H_2O
    - Pros. good thermalization efficiency (scattering with proton)
    - Cons. large absorb cross section
  - Heavy water D_2O
    - Pros. small absorb cross section
    - Cons. small thermalization efficiency (scattering with deuterium)

      D_2O is the better moderator in total
- cold neutron (20K)
  - solid heavy water (sD_2O)
    - Pros. non-inflammable
    - Cons. large binding energy of Oxygen

      Wigner energy
  - liquid Deuterium (lD_2)
    - Pros. good thermalization efficiency
    - Cons. inflammable
  - Solid heavy methane (sCD_4)
    - Pros. good thermalization (rotation and vibration)
    - Cons. inflammable

      low radiation hardness

How to produce UCN? (2)

- Doppler shifter (conventional method)
  - slow down by reflection on the moving mirror

Restriction by Liouville’s theorem

 conservation of phase space density

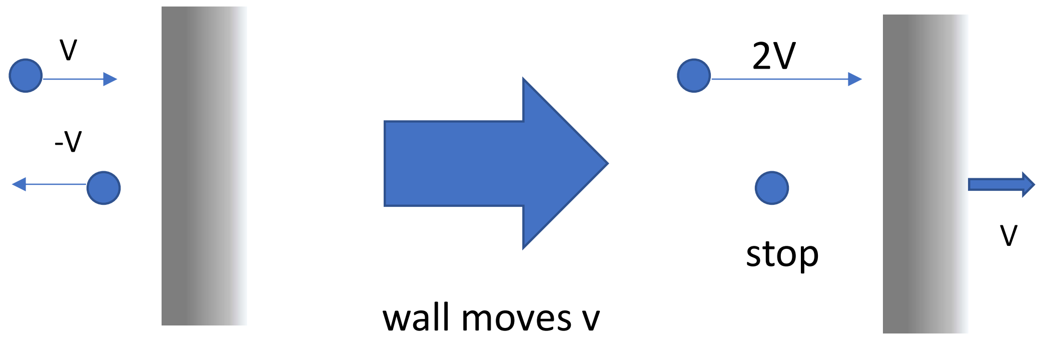

- Super thermal method (new techinic)
  - phonon up-scattering of super-fluid He or solid D2
    - use large phase space of phonon
    - free from Liouville’s theorem

UCN Source at ILL
Doppler sifter type

Institute Laue-Langevin
Grenoble, France
Reactor 57MW

UCN Production

reactor neutron ~100 meV
Liq. D_2 25K ~1 meV
vertical guide ~100 μeV → VCN
Turbine ~100 neV → UCN

Turbine UCN source

slow down by reflection on the moving mirror
Restriction by Liouville's theorem
conservation of phase space density

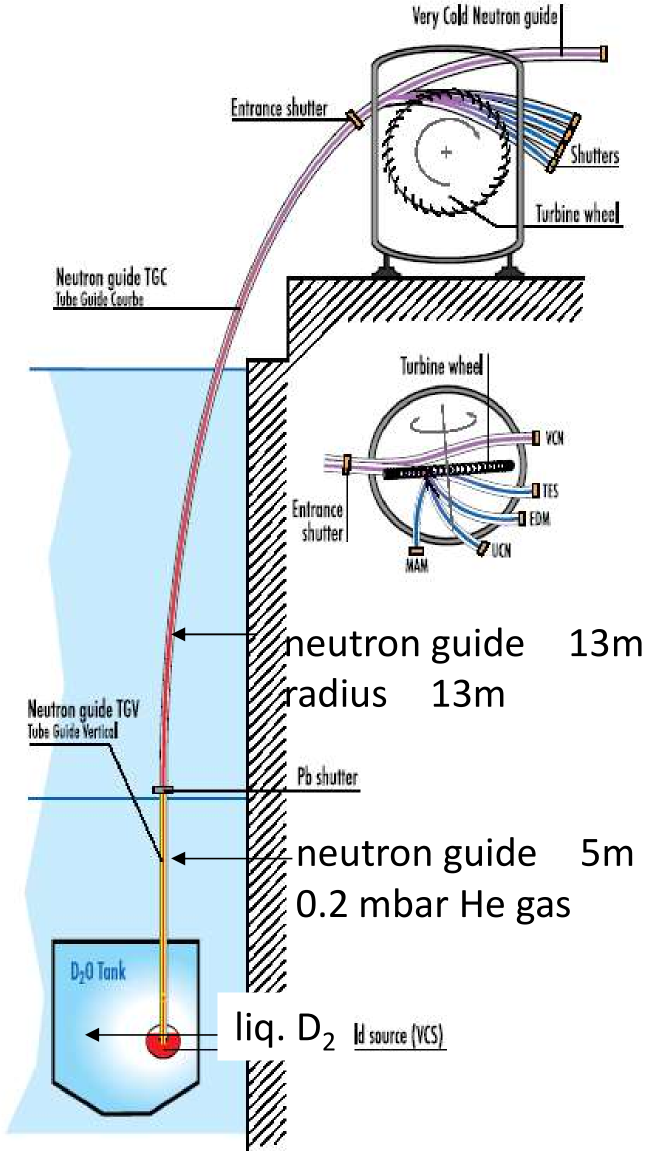

http://www.ill.fr/YellowBook/PF2

Super thermal method

- phonon down-scattering in super-fluid He or solid D_2
- use large phase space of phonon
- free from Liouville's theorem

We use superfluid helium as a UCN converter

neutron

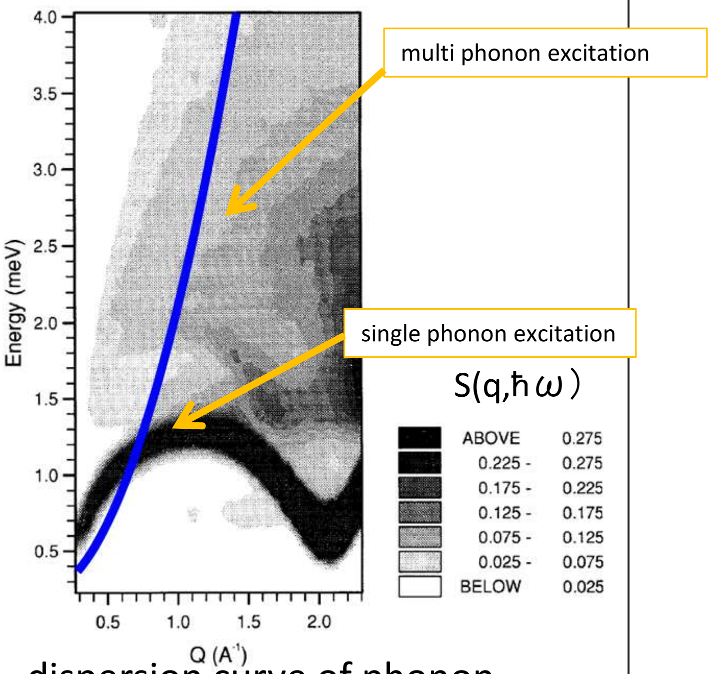

dispersion curve of phonon

M. R. Gibbs, et al
J. Low Temp. Phys. 120 (2000) 55

UCN production cross section

$$\frac{d\sigma}{dE} = 4\pi b^2 \frac{k_f}{k_i} S(q,\hbar\omega)$$

k_i, k_f : wavenumber

$S(q,\hbar\omega)$: Dynamic structure factor

resonant energy (single phonon excitation)

1 meV

UCN Production rate

$$P(E_u)dE_u = \left[\int \frac{d\Phi(E_i)}{dE} N_{\mathrm{He}} \frac{d\sigma}{dE}(E_i \to E_u) dE_i\right] dE_u$$

$$P = \int p(E_u)dE_u = N_{\mathrm{He}} 4\pi b^2 \left(\frac{\hbar}{m_n}\right)^2 \frac{k_c^3}{3}\left[\int \frac{d\Phi(q)}{dE} S\left(q, \hbar\omega = \frac{\hbar^2 q^2}{2m_n}\right) dq\right]$$

High intensity UCN source at PSI

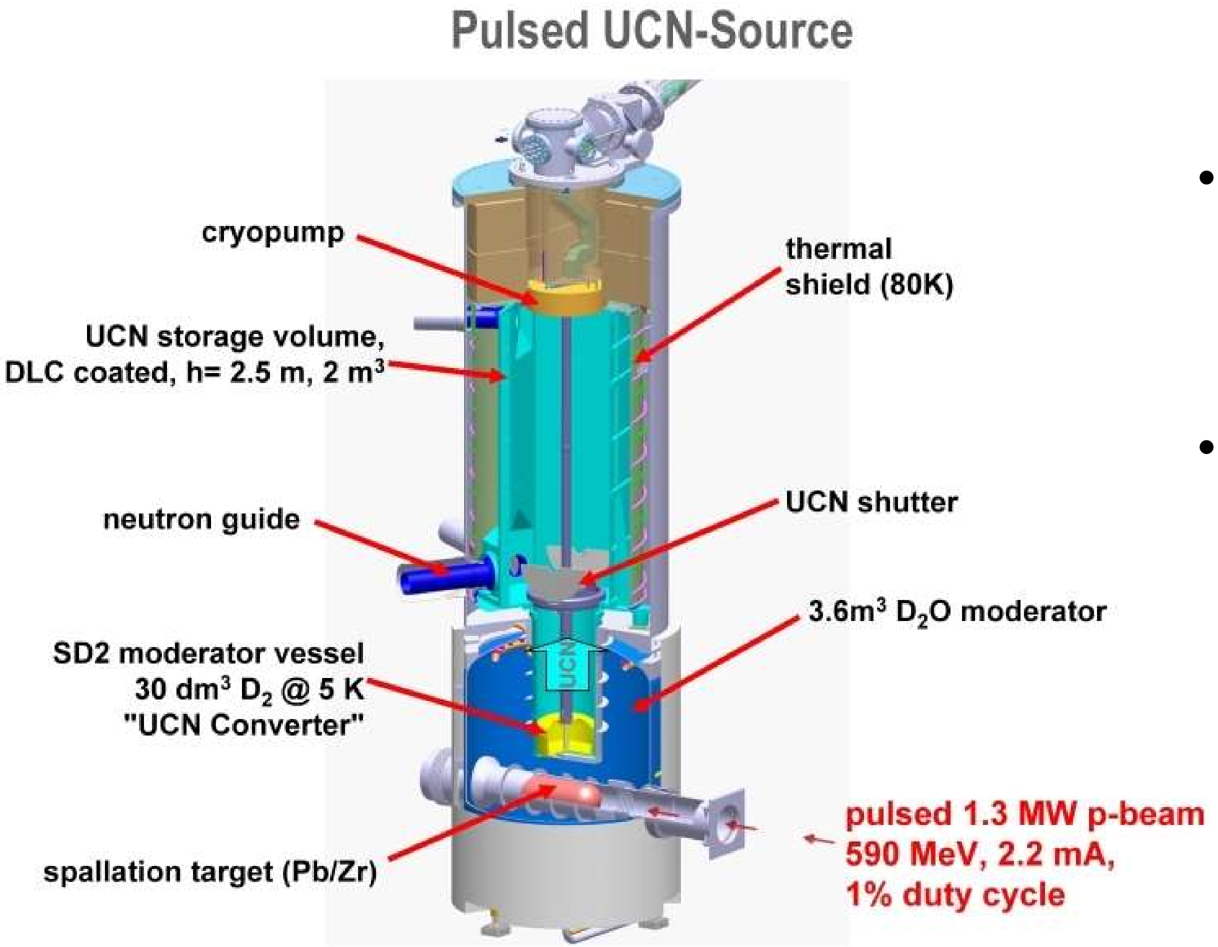

- UCN Converter
  - Solid Deuterium (SD_2)
  - Mass: 5 kg
  - Temperature: 5 K
- Proton Beam
  - power: 1.3 MW
    - 590 MeV, 2.2 mA
    - Duty cycle: 1%

nEDM measurement at ILL/PSI

experimental setup

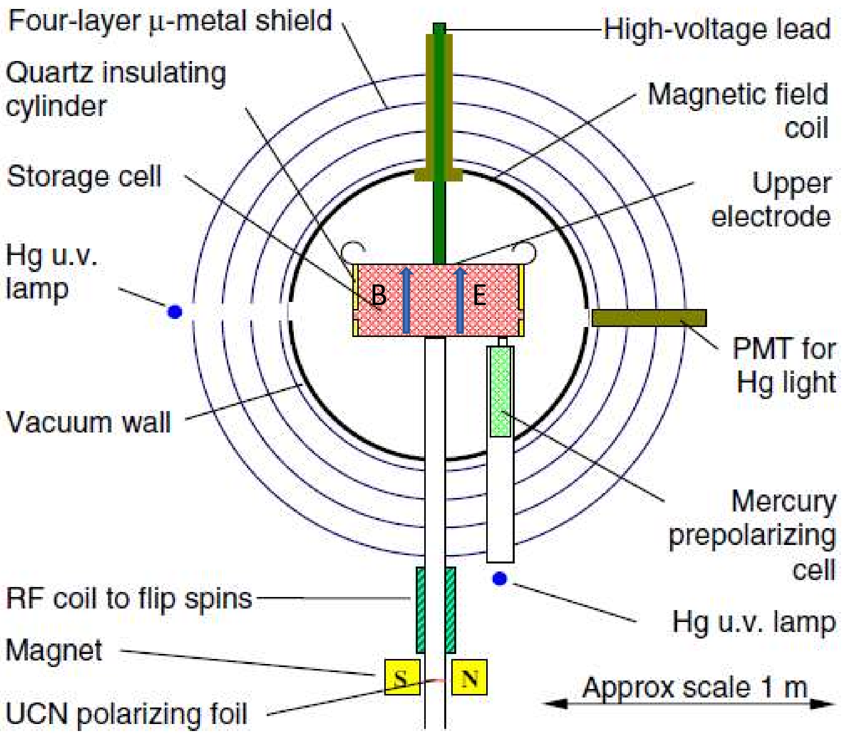

magnetic field 1μT
electric field 10kV/cm
t_c 130s

Phy. Rev. Lett. **97** .131801 (2006)

Store UCN inside of Electro-Magnetic field and measure the precession frequency by Ramsey interferometry.

1. Spin Polarizer
2. Ramsey precession
3. Spin Analyzer
4. UCN detector

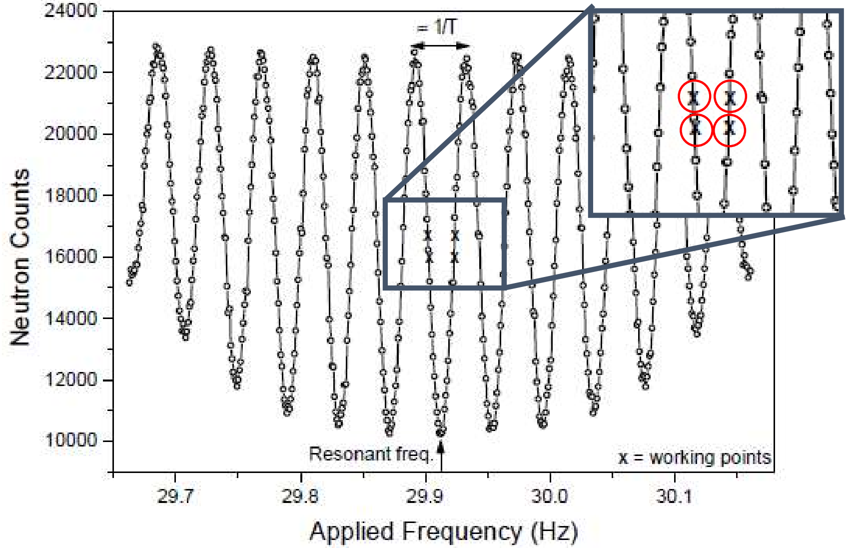

experimental setup

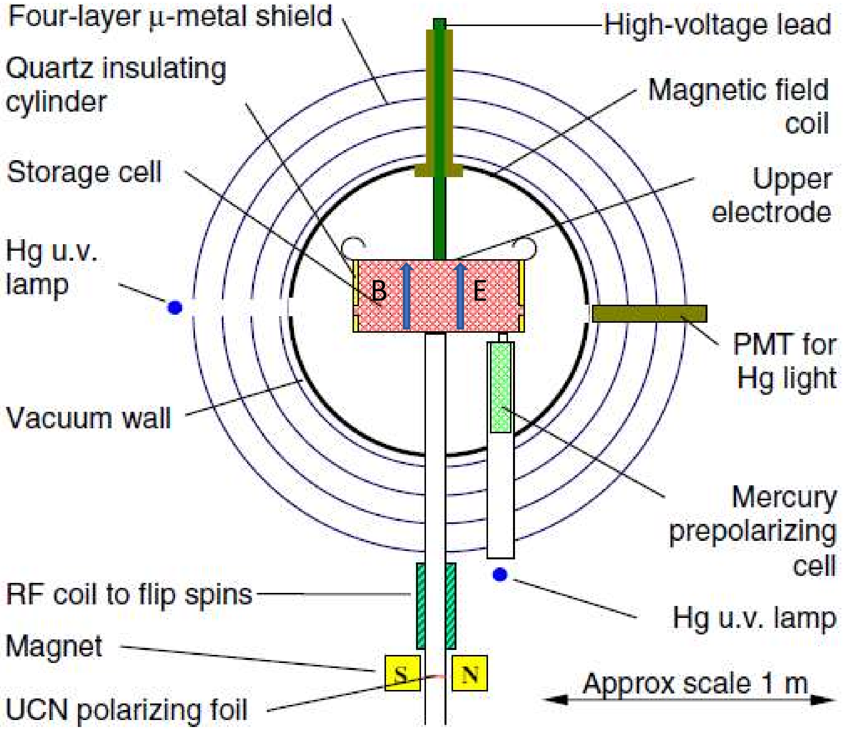

magnetic field 1μT
electric field 10kV/cm
t_c 130s

Phy. Rev. Lett. **97** .131801 (2006)

Statistical sensitivity

$$\sigma_d = \frac{\hbar}{2\alpha E t_c \sqrt{N}}$$

α : polarization (isibility)
E : electric field
t_c : precession time
N : number of UCN

The new result reported in 2020
$d_n=(0.0 \pm 1.1_{stat} \pm 0.2_{sys}) \times 10^{-26}$ e.cm
@ PSI
upper limit
1.8×10^{-26} ecm (90% C.L.)

Statistically limited
–> necessity of high intensity UCN source

co-magnetometer

reduce systematic error by magnetic field stability

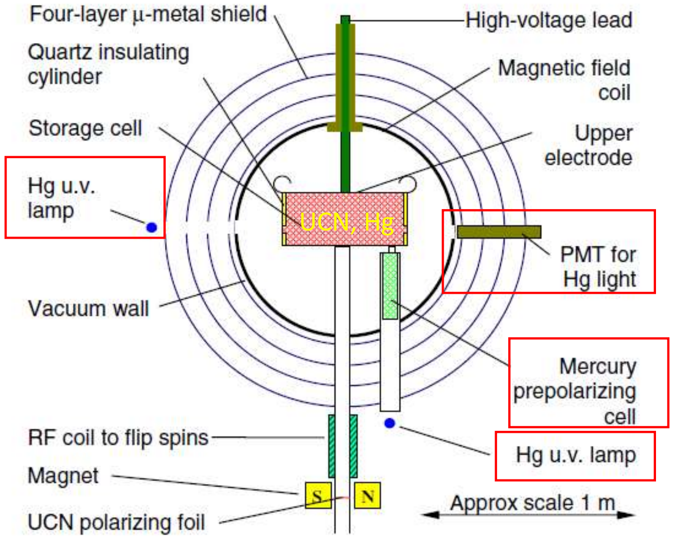

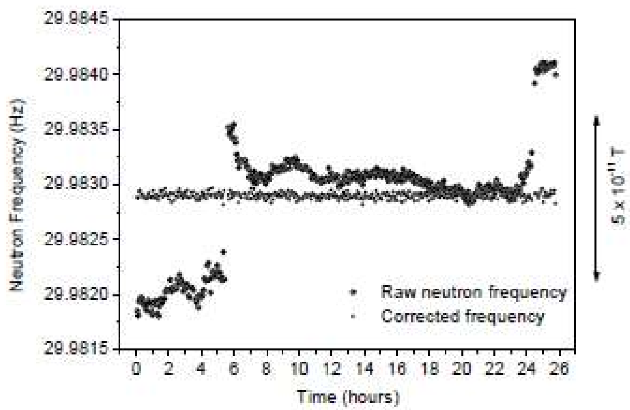

P. G. Harris *et al.*, Phys. Rev. Lett. **82**, 904 (1999).

frequency shift

$$\Delta\omega = 4 \times 10^{-7} Hz$$

(E = 10kV/cm, d = 10^{-27}ecm)

cf. Larmor frequency of neutron

30Hz @ B_0 = 1μT

required magnetic field stability : 10^8

1μT * 10^{-8} = 10 fT

It is difficult to stabilize magnetic field in such a accuracy

-> monitor and correct magnetic field

^{199}Hg for co-magnetometer

- feels same magnetic field as UCN
- polarization is measured by UV laser

Geometric Phase effect　現在の系統誤差の最大要因

- 水平方向磁場による周波数シフト(Bloch-Siegert shift)

$$\Delta\omega = \frac{{\omega_{xy}}^2}{2(\omega_0 - \omega_r)}$$

ω_r: angular speed of B_{xy} rotation

- 水平方向磁場

$$B_{xy} = \frac{\partial \mathrm{B_z}}{\partial \mathrm{z}}\frac{R}{2} + \frac{E\times v}{c^2}$$

  - 第1項： 磁場非一様性
  - 第2項: 相対論的運動
- UCNの載っている座標から見るとBxyは回転しているように見える
- 右、左回りで第2項のみ符号を変える

$$\Delta\omega_{ave} = \frac{1}{2}\frac{\gamma B_z\left[\left(\gamma\frac{\partial B_z}{\partial z}\frac{R}{2}\right)^2 + \left(\frac{v_\phi E_z}{c^2}\right)^2\right] + \gamma^2\frac{\partial B_z}{\partial z}\frac{R}{2}\frac{v_\phi \boxed{E_z}}{c^2}}{(\gamma B_z)^2 - (v_\phi/R)^2}$$

電場反転の際の周波数差を取った際にEに比例する項が残る

偽EDM

電場反転したときの周波数差

$$d_{false}^{GPE} \approx \frac{\hbar\gamma^2\frac{\partial B_z}{\partial z}{v_\phi}^2 R^2/c^2}{(\gamma B_z)^2 - (v_\phi/R)^2}$$

$\frac{\partial B_z}{\partial z} = 1\ \mathrm{nT/m}$ correspond error of 10^{-26} ecm

磁場の一様性を高めることが重要

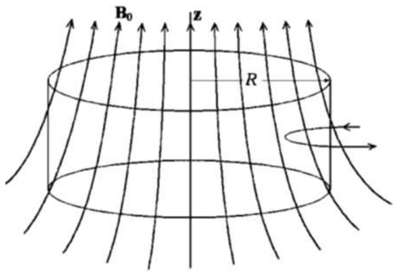

FIG. 1. (Color online) The shape of the $\mathbf{B}_0$ field lines, when there is a positive gradient $\partial B_{0z}/\partial z$, shown in relation to an outline of the trap used to store ^{199}Hg atoms and UCN's for the neutron EDM measurements at the ILL. If another field is superimposed having lines that both enter and leave through the sidewalls, like the one on the right-hand side, it will be shown later that it does not affect the false EDM signals that are generated.

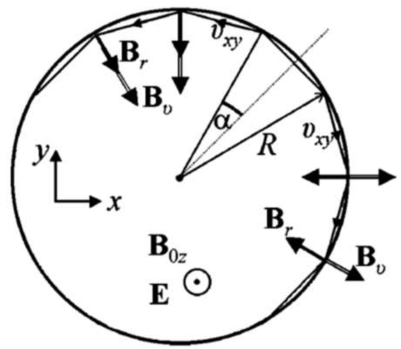

FIG. 3. (Color online) A view of the xy plane of the trap bounded by the circular sidewall. Part of an orbit is shown projected onto the xy plane for a particle undergoing specular reflection. The orbit is characterized by the angle α. Vectors $\mathbf{E}$ and $\mathbf{B}_{0z}$ point towards the reader and $\partial B_{0z}/\partial z$ is positive.

Pendlebury et al, PRL 70, 032102 (2004)

nEDM measurement at PSI

data accumulation

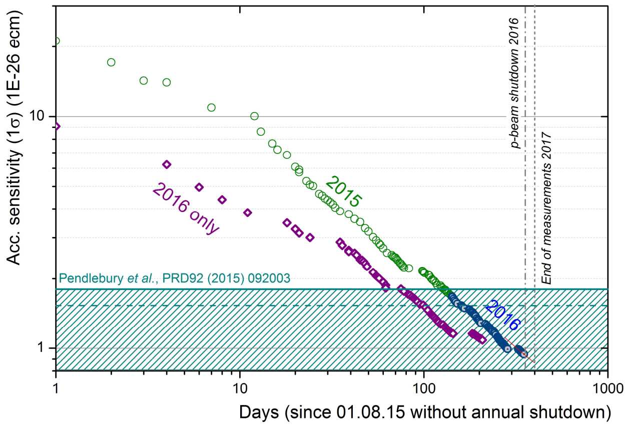

- Basically same setup as ILL experiment
  - Cell volume : 20 L
- 11400 UCN are counted per cycle
- data taken: 2015 – 2016
  up to reach 1×10^{-26} ecm statistical error
- Blind analysis by two groups

statistically limited

$$d_n = (0.0 \pm 1.1_{stat} \pm 0.2_{sys}) \times 10^{-26}\ \text{ecm}$$
$$|d_n| < 1.8 \times 10^{-26}\ \text{ecm (90\% C.L)}$$

C. Abel, et al, Phys. Rev. Lett. 124 81803 2020

Typical data cycle

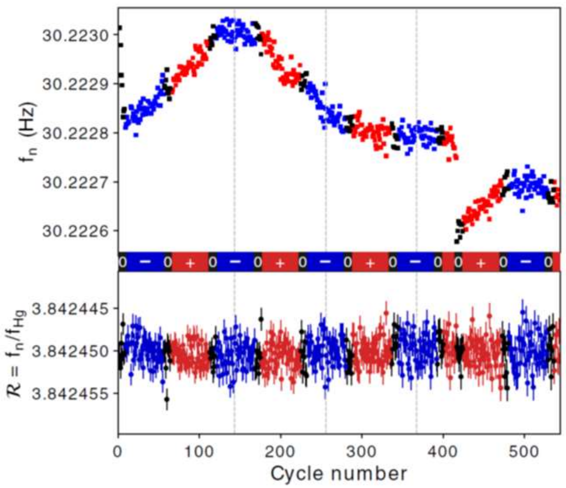

resonant frequency of neutron

E

correction by co-magnetometer

TABLE I. Summary of systematic effects in 10^{-28} e.cm. The first three effects are treated within the crossing-point fit and are included in $d_\times$. The additional effects below that are considered separately.

Effect	Shift	Error
Error on $\langle z \rangle$	...	7
Higher-order gradients $\hat{G}$	69	10
Transverse field correction $\langle B_T^2 \rangle$	0	5
Hg EDM [8]	−0.1	0.1
Local dipole fields	...	4
$v \times E$ UCN net motion	...	2
Quadratic $v \times E$	...	0.1
Uncompensated G drift	...	7.5
Mercury light shift	...	0.4
Inc. scattering ^{199}Hg	...	7
TOTAL	69	18

systematic error

PSI次期計画 n2EDM

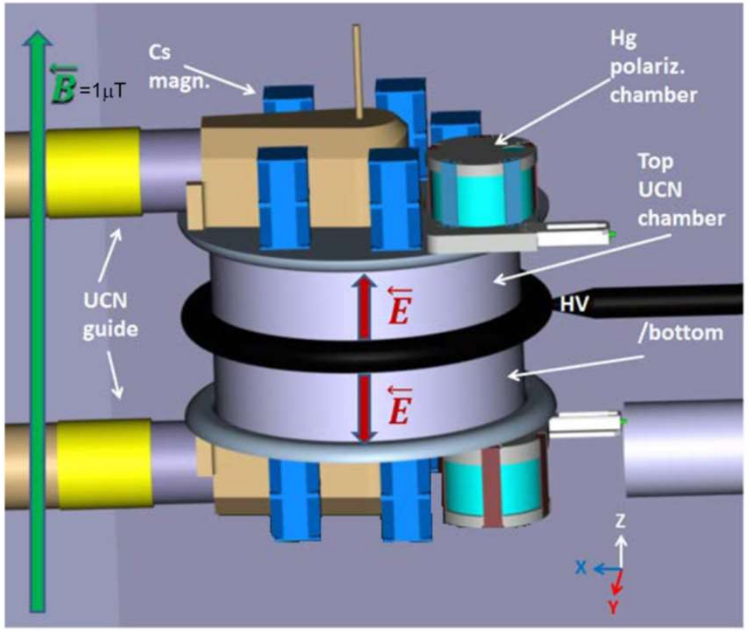

統計精度向上

- UCN密度は現行のまま
- 容器直径を大きく

  47 cm → 80 cm

系統誤差を抑えるのが課題

- 上下対称セルを用いて磁場ドリフトの影響をキャンセル
  - 同時に統計の増加にも寄与
- 磁気シールドルームを新設

	Current	n2EDM	n2EDM	n2EDM	n2EDM	n2EDM	n2EDM
phase	2016 average	comm.	comm.	meas.	meas.	meas.	meas.
ID (cm)	47	47	47	80	80	100	100
coating	dPS	dPS	iC	dPS	iC	dPS	iC
α	0.75	0.8	0.8	0.8	0.8	0.8	0.8
E (kV/cm)	11	15	15	15	15	15	15
T (s)	180	180	180	180	180	180	180
N	15′000	50′000	100′300	121′000	292′000	160′000	400′000
$\sigma(d_n)$ (e·cm) per day	11×10^{-26}	4.1×10^{-26}	2.8×10^{-26}	2.6×10^{-26}	1.7×10^{-26}	2.3×10^{-26}	1.4×10^{-26}
$\sigma(d_n)$ (e·cm) 500 data days	5.0×10^{-27}	1.8×10^{-27}	1.3×10^{-27}	1.2×10^{-27}	7.5×10^{-28}	1.0×10^{-27}	6.4×10^{-28}

B. Lauss, nEDM2017

統計誤差の改善

現在の観測感度は統計誤差によってリミット

→ 観測するUCNの個数を増やす

1. 観測容器を大きくする

PSIの次期計画はこの方法

容器直径　47 cm → 80 cm

容器内の磁場の安定性・一様性を保つのが困難

2. UCN密度を増大させる

大強度超冷中性子源の開発

UCN密度 ～ 1 UCN/cm^3 → 250 UCN/cm^3

PSI　TUCAN

TUCANによる高強度UCN源開発

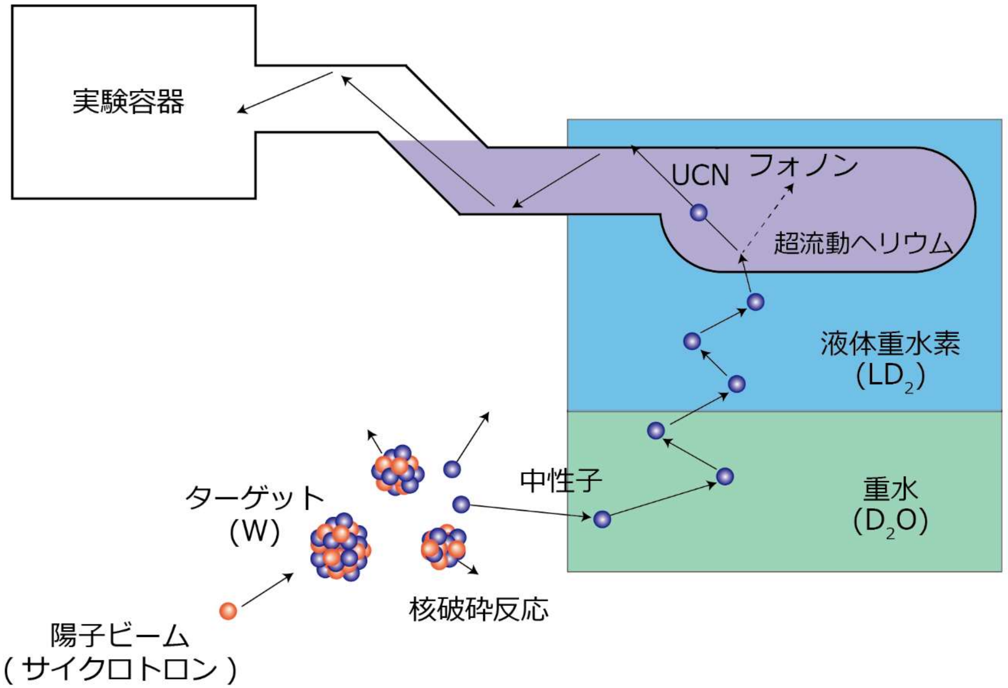

核破砕中性子　～ MeV

↓ D_2O/LD_2 モデレータ (300K, 20K)

冷中性子　　～ meV

↓ Phonon scattering in He-II

超冷中性子　～100neV

特徴

・加速器中性子　(核破砕反応)

高い冷中性子束

標的とHe-IIの距離を近くできる

高い熱負荷

・UCNコンバータ : 超流動ヘリウム

長い蓄積時間

中性子寿命:フォノンによるup-scattering

$(\tau_s \propto T^{-7})$

τ_s = 36 s at $T_{He\text{-}II}$ = 1.2 K

τ_s = 600 s at $T_{He\text{-}II}$ = 0.8 K

(Cf. SD_2 : T_s = 24ms)

高い熱負荷の下で超流動ヘリウムを
低温に保ち続けることが重要

UCN Storage time

UCN production rate

$$\frac{d\rho_{UCN}}{dt} = P - {\rho_{ucn}}/{\tau}$$

P : UCN production rate

τ : Storage time

UCN density

ρ = Pτ (1 – exp(-t/τ)) ∝ Pτ

long τ is important

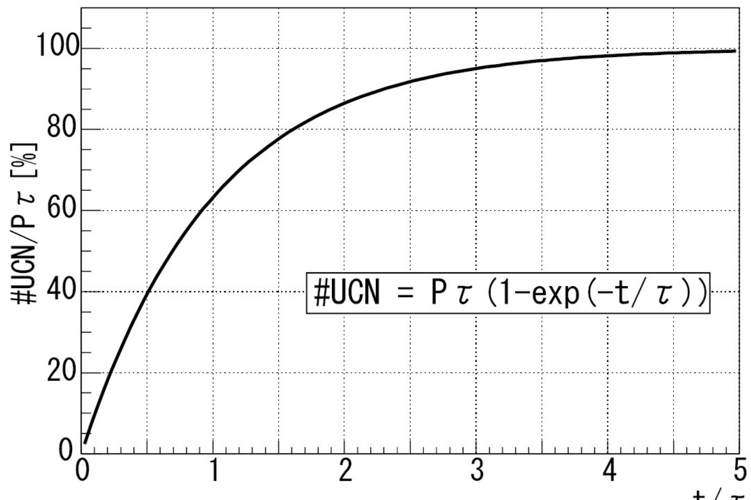

UCN density during proton irradiation

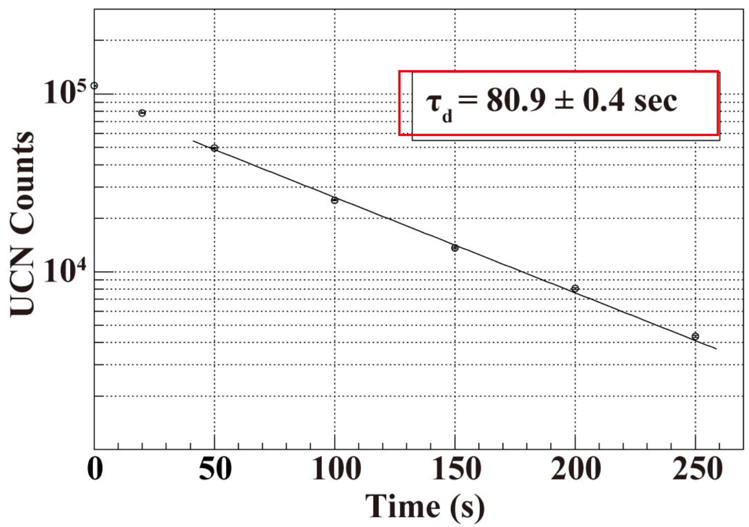

UCN Storage Life Time

$${1}/{\tau} = {1}/{\tau_{phonon}} + {1}/{\tau_{abs}} + {1}/{\tau_{wall}} + {1}/{\tau_{\beta}}$$

τ_{abs} : absorption by ^{3}He > 1000 s

purification to ^{3}He/^{4}He <10^{-11}

τ_{phonon}: phonon up-scattering T 〜 1.0 K

τ_{wall} : wall loss clean surface

τ_{β} : β decay (886s)

Purification of ^{4}He by Heat Flush Method

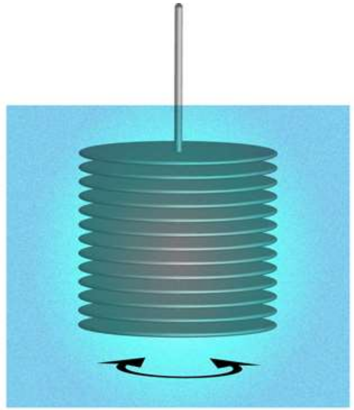

Two Fluid Model

	Normal fluid	Superfluid
Viscosity	H_n	$\eta_s = 0$
Entropy	S_n	$S_s = 0$

Heat Flush

When heat apply,

- zero entropy superfluid is converted to be entropy-carrying normal fluid
- Normal fluid excess around heater
- Counter flow
  - Normal mode (^{3}He) : away from the heater
  - Super mode : towards to the heater

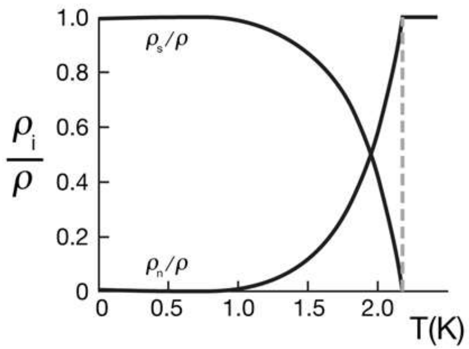

10.1103/Physics.3.5

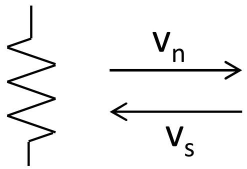

Heater

^{3}He/^{4}He $<10^{-11}$ is achievable by heat flush method

P.C. Hendry and P.V.E. McClintock, Cryogenics 1987 Vol 27

Helium-3 cryostat

- to keep He-II temp. ～ 1.0 K
- decompressed Helium 3
  - use latent heat of evaporation
- ^{3}He vs ^{4}He
  - vapor pressure @ 0.8K
    - ^{3}He: 3 Torr
    - ^{4}He: 0.01 Torr
  - cooling power

    @ 0.8K with 10, 000 m^3/hour pumping
    - ^{3}He: 15W
    - ^{4}He: 0.13 W

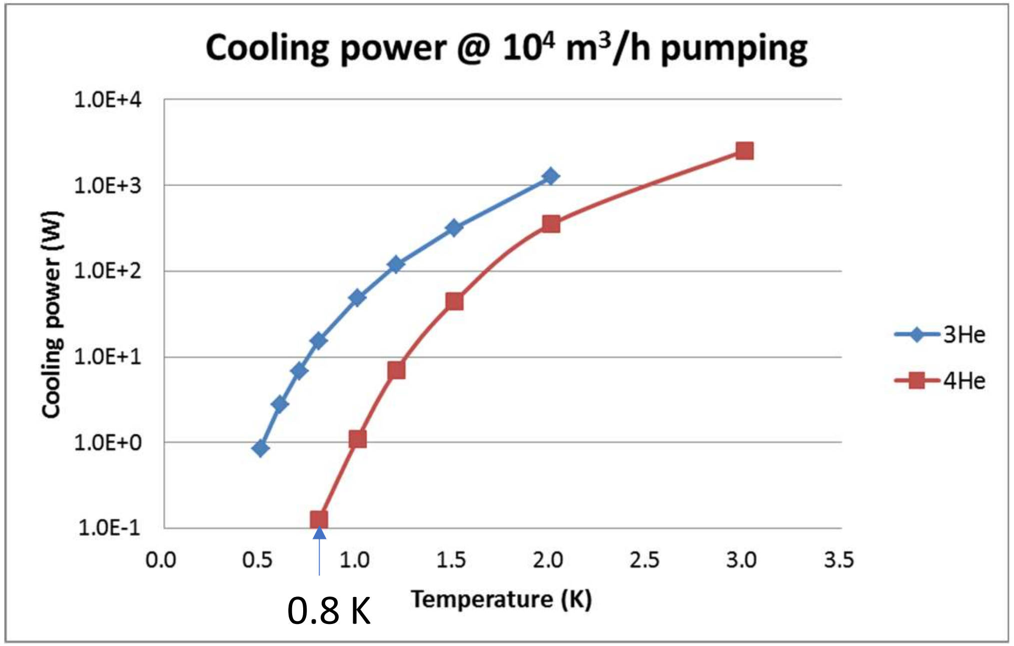

プロトタイプUCN源

- RCNPでの原理検証
  - 加速器中性子＋超流動ヘリウムコンバーターの組み合わせとして世界唯一
  - 陽子ビーム強度

    400 MeV × 1 μA = 0.4 kW
  - UCN密度　9 UCN/cm^3 @ UCN源
    - Y. Masuda et al., Phys. Rev. Lett. 108, (2012), 134801

- TRIUMFへ移設 (2016年ー)
  - UCN源専用陽子ビームラインにおいてUCN生成に成功
  - 陽子ビーム最大強度

    500 MeV × 40 μ A = 20 kW

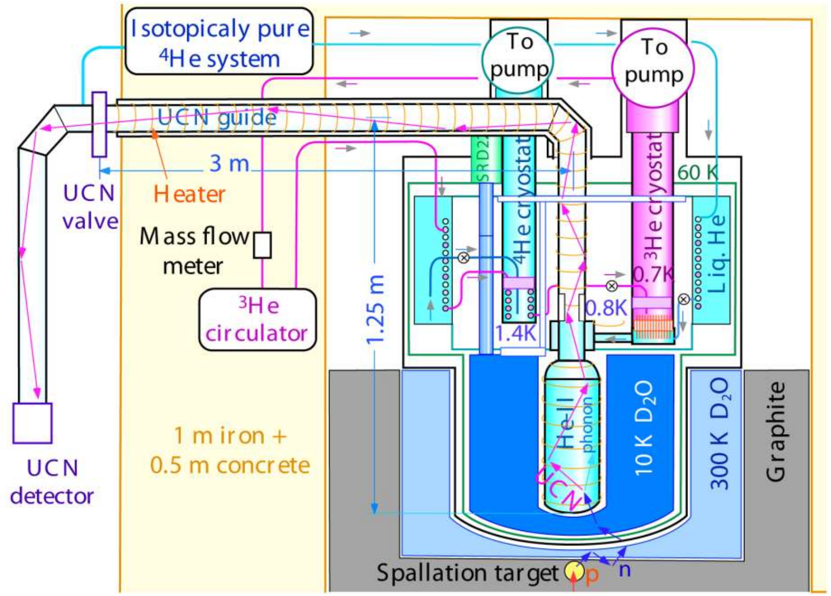

Improvement of UCN Storage time

Year	τ_s	T_{HeII}	Improvement
2002	14 s	1.2K	
Jun 2006	29 s	0.9K	Use ^{3}He cryostat
Nov 2006	34 s	0.8K	Reduce HeII film perimeter (8.5 cm → 5 cm)
Jul 2007	39 s	0.8K	Remove ^{3}He contamination
Apr 2008	47 s	0.8K	Fomblin coating
Dec 2009	61s	0.8K	Alkali cleaning
Feb 2011	81s	0.8K	High temperature baking (140℃)

UCN Source @ TRIUMF

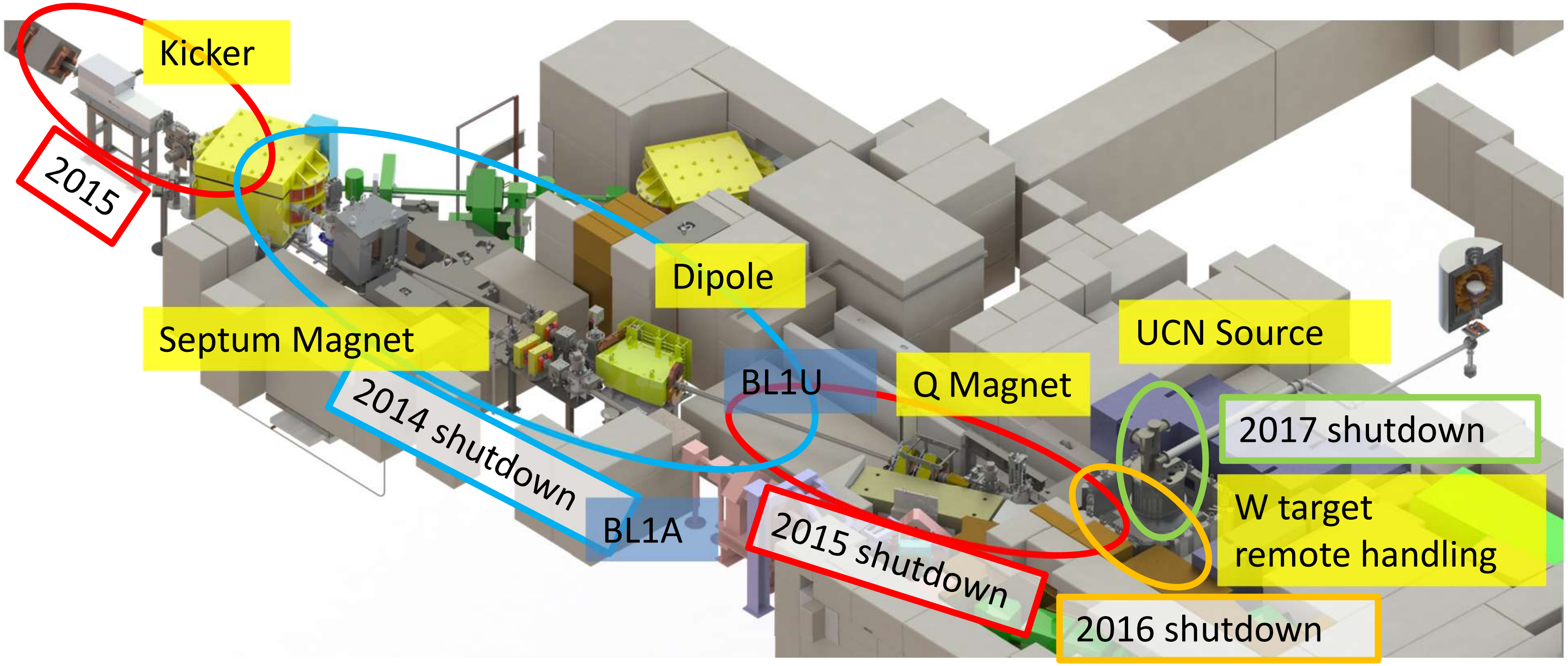

Major Milestone

- ✓ ～2016 springdedicated proton beam line for UCN(BL1U 500MeV, 40μA completed
- ✓ 2016 fall commissioning for proton beam line & cold neutron production succeeded
- ✓ 2017 - 2019 UCN production by the prototype UCN source 1 month /year
- 2021 - Upgrade UCN source

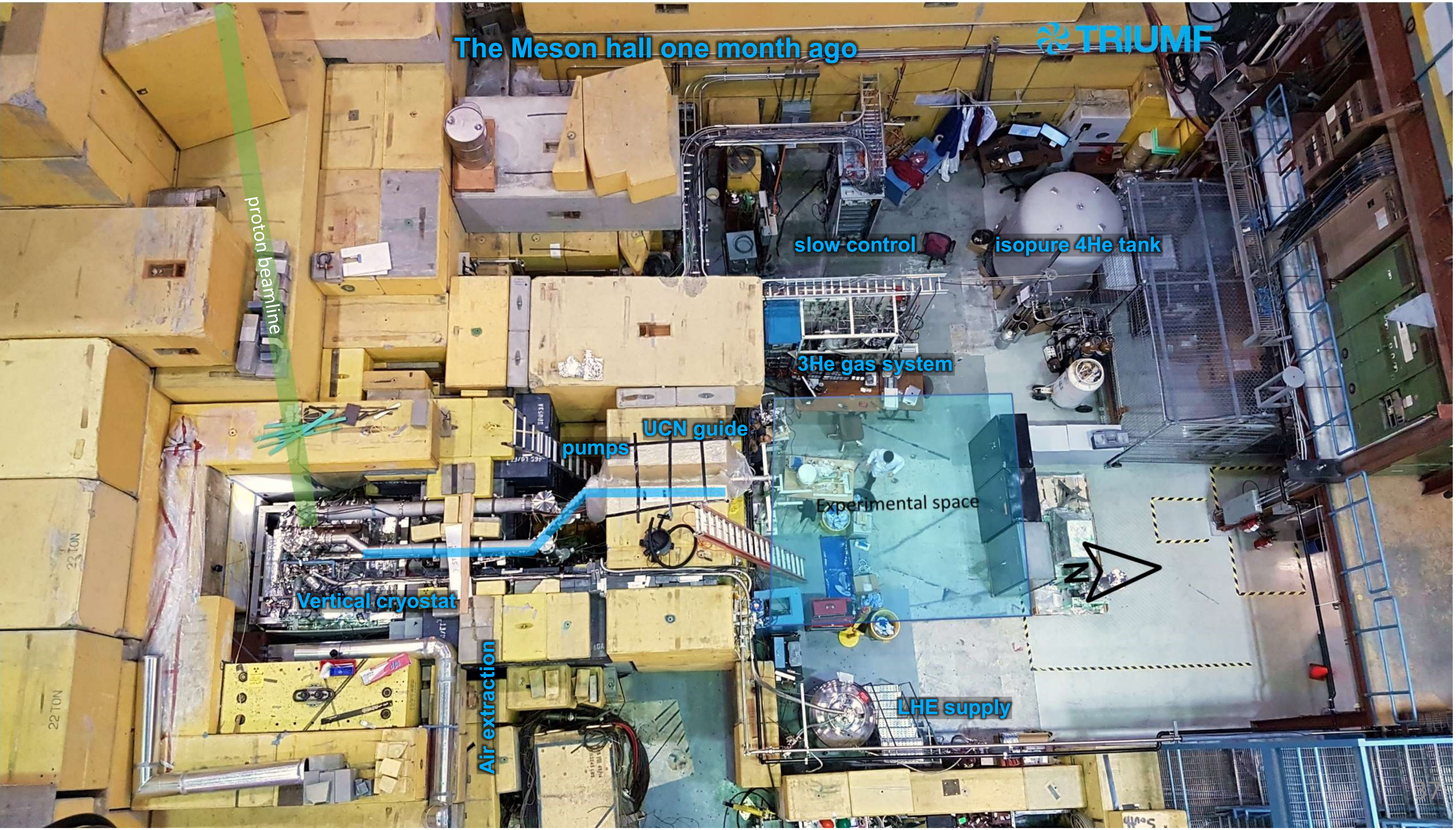
The Meson hall one month ago
TRIUMF
proton beamline
slow control
isopure 4He tank
3He gas system
UCN guide
pumps
Experimental space
N
Vertical cryostat
Air extraction
LHE supply

UCN production with the prototype source

- **Nov 13, 2017: first UCN produced at TRIUMF**
- 2017 – 2019 : UCN production
  - 1 month/year
- Experimental program
  - source and UCN hardware characterization
- UCN source performance
  - For 60 sec proton beam irradiation
    - Approx. 5×10^4 per shot at 1 μA
    - $> 3 \times 10^5$ at 10 μA
  - Storage life time : 35 sec

    (81 sec at RCNP)
- Cooling power is not enough
  - UCN yield is not proportional to the beam current
  - Temperature of He-II increase

陽子ビーム出力を上げると超流動ヘリウム温度が上がり、取り出せるUCN数が減る

冷凍機能力の限界

Timing spectrum

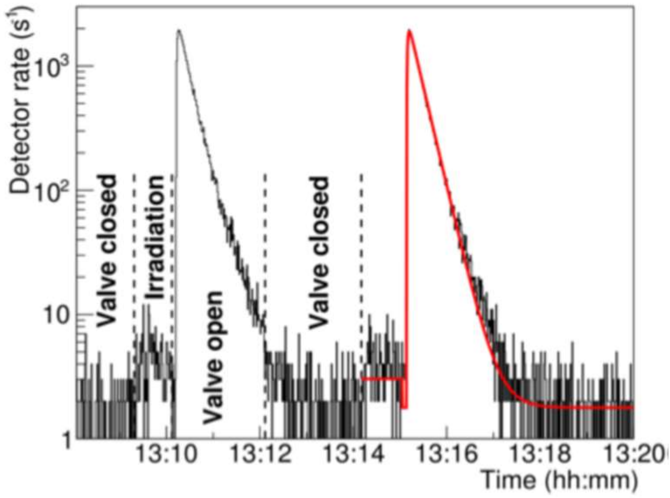

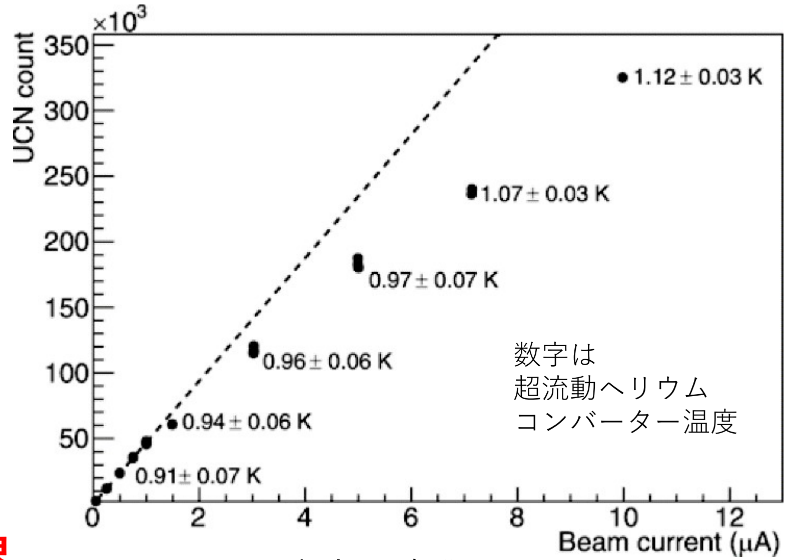

陽子ビーム出力を変化させたときの
UCNカウント数の変化

UCN 源アップグレード

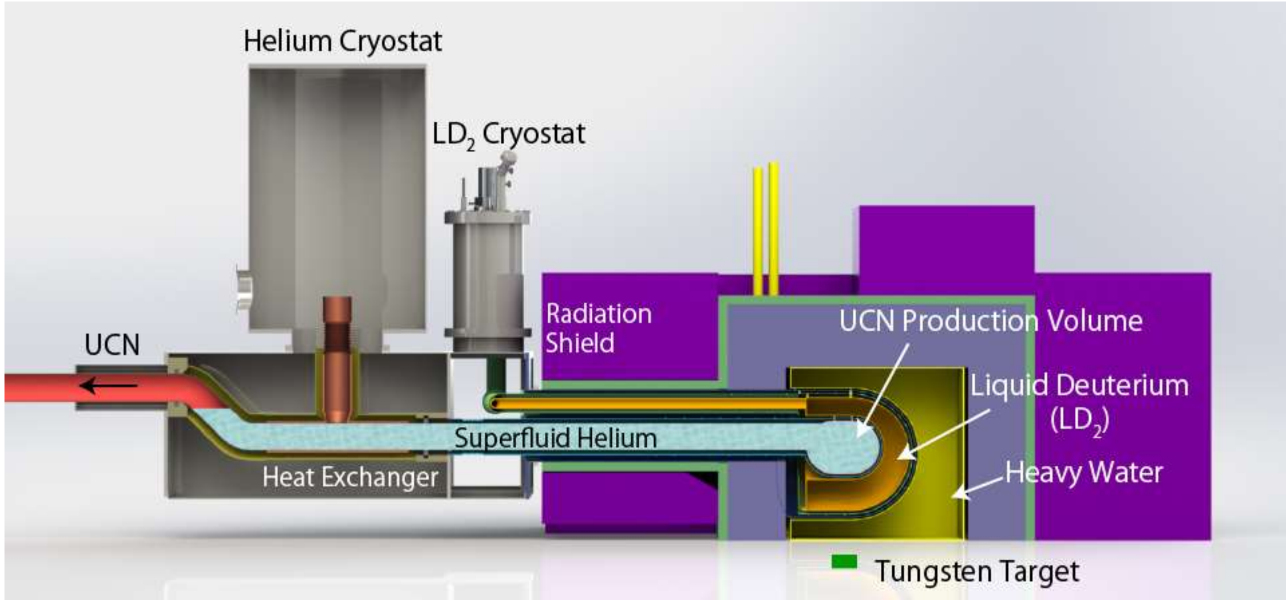

- 液体重水素(LD_2)モデレーター
  - 冷中性子フラックスの増加　(×2.5)
- 高い冷凍能力を持つヘリウム冷凍機
  - 超流動ヘリウムコンバーター体積の増加 (×3)
  - 陽子ビームーパワー増強　(×50)
    - 0.4 kW at RCNP -> 20 kW at TRIUMF
  - 超流動ヘリウムにかかる熱負荷
    - 8.1 W　(容器の発熱を含む)

LD2 Moderator

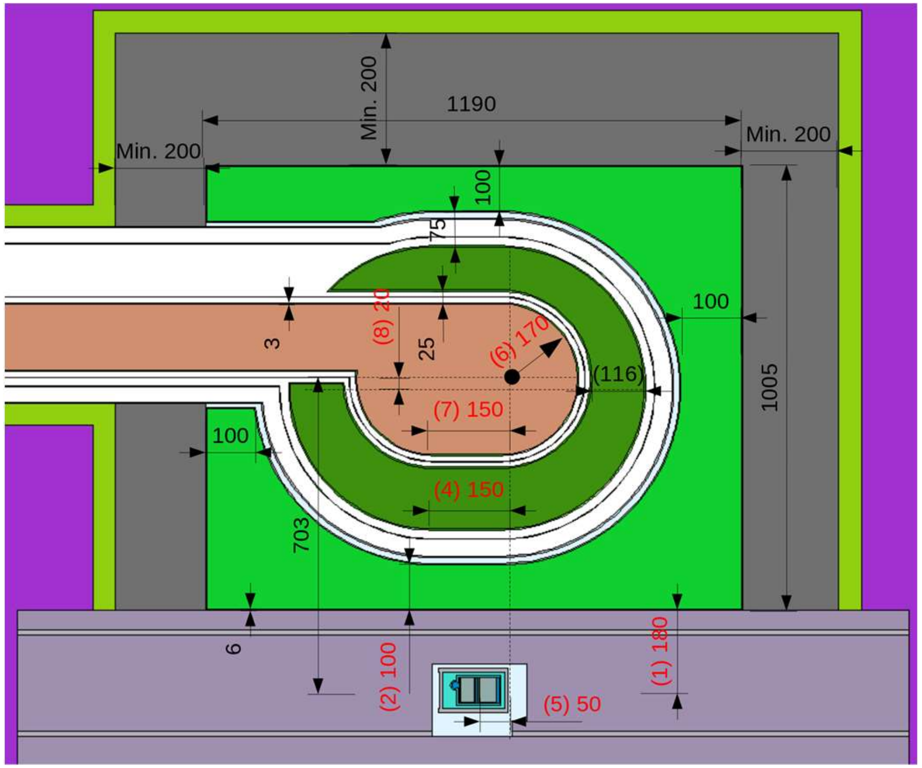

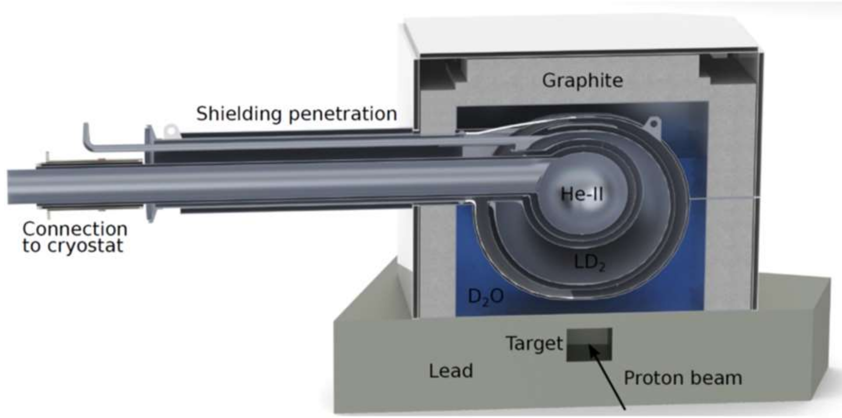

Detailed engineering model

- Minimized wall thicknesses with ANSYS
- Minimized cost for D_2O (430 + 200 L) and graphite (reused)
- Optimized position above target
- **UCN production: 1.4·10^7 to 1.6·10^7 UCN/s**
- **Max. heat load: 8.1 W @ 1.1 K**
- 27 L He-II converter (+ ~50 L in guide)
- 125 L LD_2, max. heat load 63 W @ 20 K
- Storage lifetime in source: ~30 s
- Recently published: [10.1016/j.nima.2020.163525](https://doi.org/10.1016/j.nima.2020.163525)

LD2 vs D20

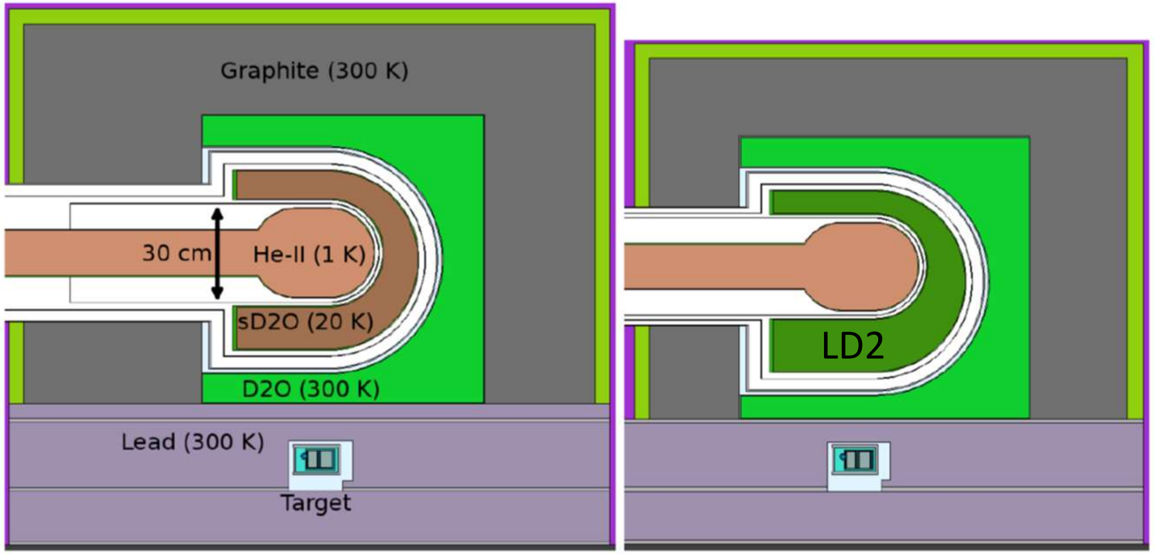

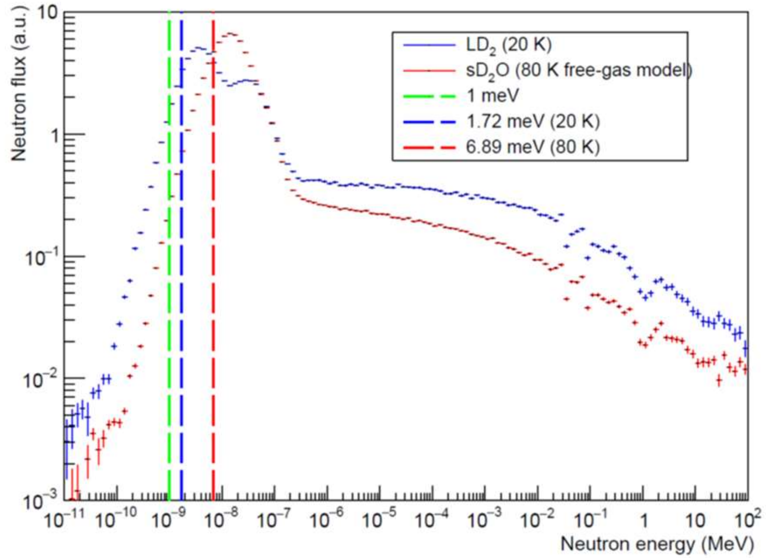

neutron flux

	sD_2O	110 l LD_2	200 l LD_2
UCN production at 5 W heat load (s^{-1})	$0.40 \cdot 10^7$	$\boxed{1.02 \cdot 10^7}$	$1.33 \cdot 10^7$
Heat load at 40 μA (W)	5.1	7.6	5.4
Thickness of lower cold-moderator layer (cm)	14.0	17.5	23.1
Thickness of upper cold-moderator layer (cm)	9.3	7.5	15.8
Heat load on cold moderator at 40 μA (W)	60.5	50.0	36.7

factor 2.5 improvement

Superfluid helium UCN converter cooling

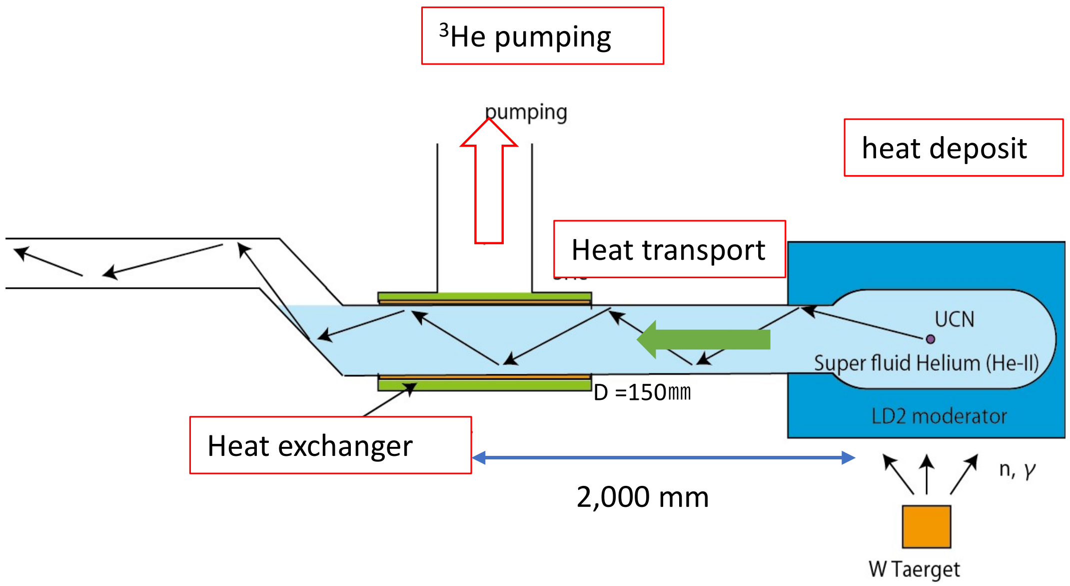

$$T_{prod} = T_{3He} + \underbrace{\Delta T_{3He\text{-}Ni} + \Delta T_{Ni\text{-}HeII}}_{\text{Kapitza cond.}} + \Delta T_{HeII}$$

^{3}He pumping

Heat transfer in He-II

Components

1. Helium-3 cryostat
   - Have to be placed behind radiation shield
     - L = 2.0 m
   - High cooling power : ～11 W @1.0K,
     - 10 W: beam, 1 W: static
2. Heat Exchanger design
   - Kapitza conductance
3. Heat transport in superfluid helium
   - Flow pattern
     - Superfluid turbulent
     - Gorter-Millink heat transfer

1. Helium-3 cryostat

- 液体ヘリウム３減圧により1 K以下へ
  - 10 W @ 0.8 K
  - 飽和蒸気圧: 380 Pa @ 0.8 K
- ヘリウム3循環
  - ヘリウム3は貴重
    - 30万円 / 1L gas
  - 3つの液相・多段の熱交換器
    - 4.2K 液体ヘリウム4
      - 大気圧
    - 1.6 K 液体ヘリウム4
      - JT膨張 -> 750 Pa
    - 0.8 K 液体ヘリウム3
      - JT膨張 -> 380 Pa
    - 熱交換器
      - 気体の潜熱を有効活用

次ページへ

  - mass flow rate
    - 1.14 g/sec for 10 W cooling power

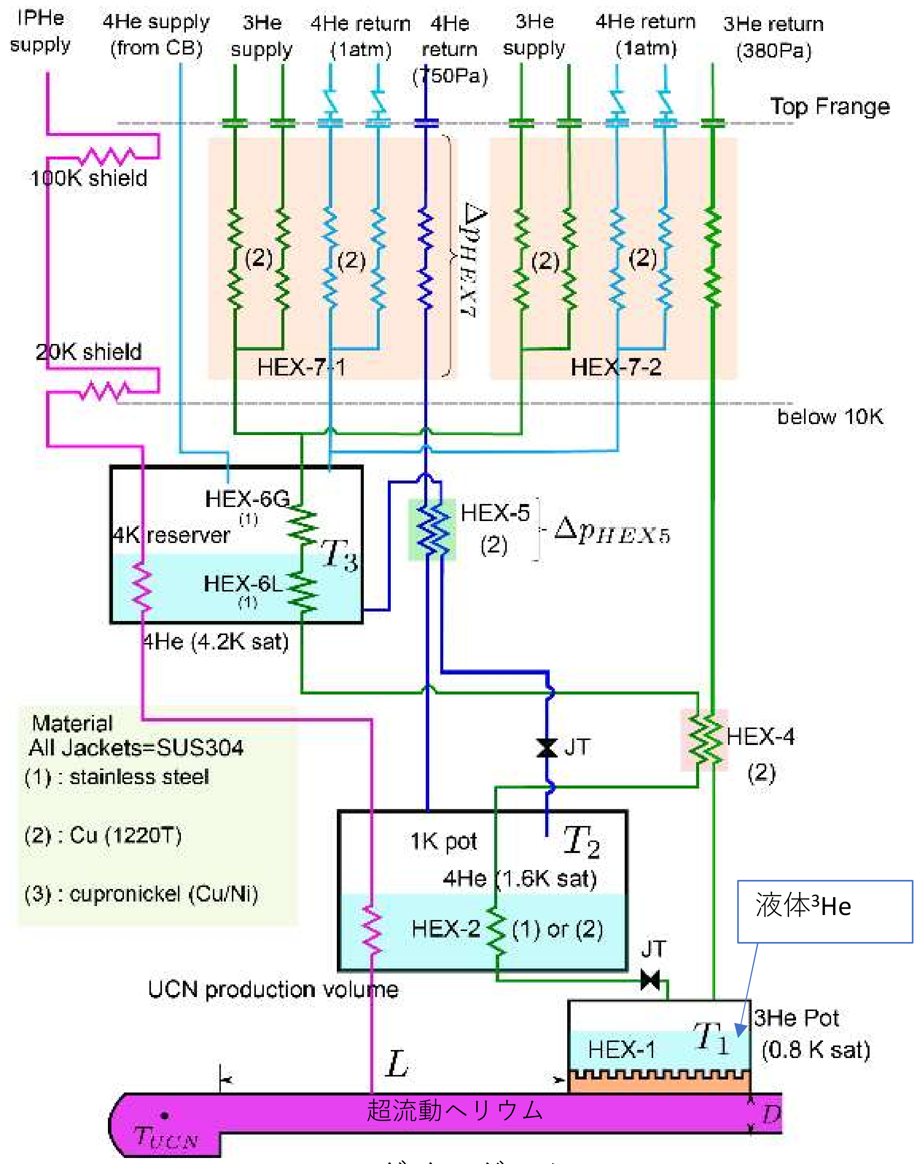

フローダイアグラム

1. Helium-3 cryostat

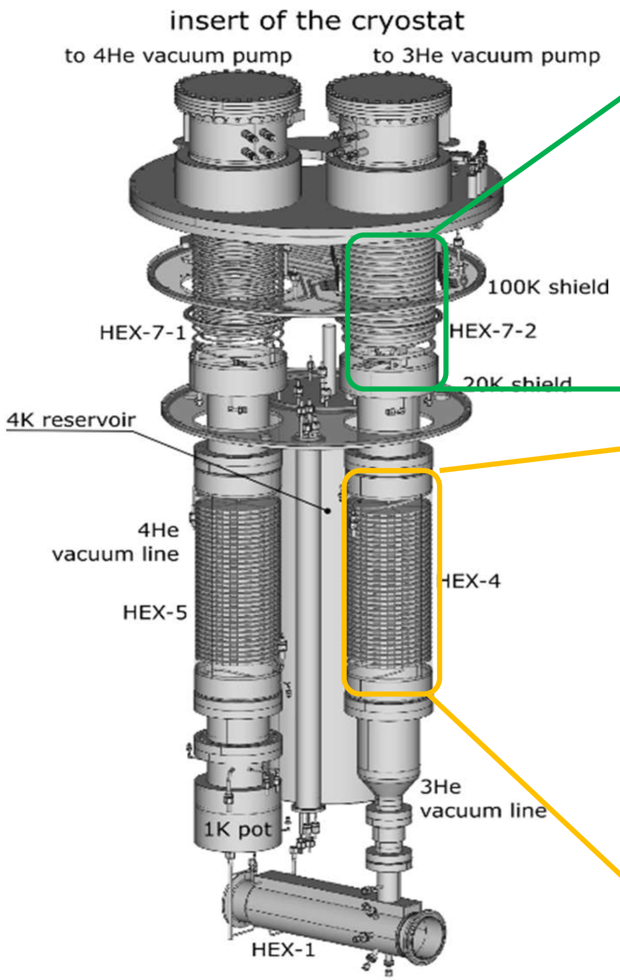

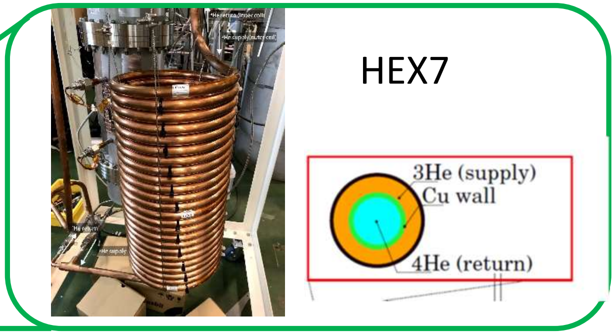

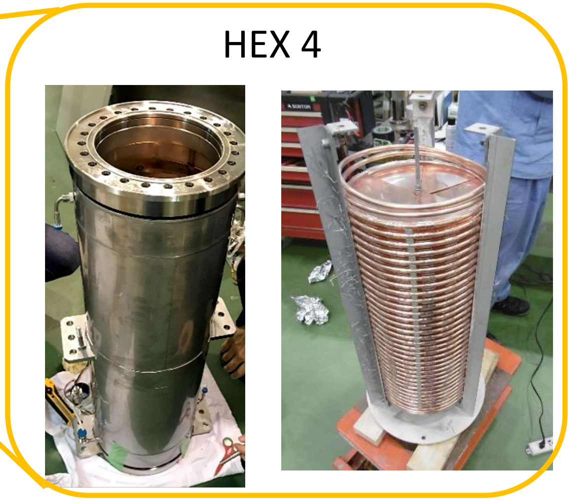

多段の熱交換器

　気体の潜熱を用いて有効的にシステムを冷却する

- HEX7
  - 常温の気体ヘリウム3を4Kヘリウム槽からの蒸発ガスで冷やす
    - 3He: 300 K -> 10 K
    - 3He エンタルピー
      - 2,074 J/g @ 300 K
      - 75 J/g @ 10 K

      約30倍
  - 2重管構造
  - スペース削減のため3He, 4He排気管の中に設置
    - １K pot, 3He potの蒸発ガスの潜熱も有効利用
- HEX4 & HEX5
  - 4Kの3He or 4Heを3He pot or 1K potの蒸発ガスで冷やす
  - JT液化効率(4He)

    JT膨張の後にどれだけ液として残るか
    - 4.2 K -> 1.6 K　　59%
    - 2.8 K -> 1.6 K　　79 %

大型ヘリウム3冷凍機開発

ヘリウム3冷凍機

- 設計

  冷却能力とヘリウム4消費量のバランス

  - 冷凍能力　　　　10 W @ 0.8 K
  - 液体ヘリウム4消費量　　< 40 L /hour

- 製作
  - 熱交換器

    組み込み前の性能試験

  - 全体組み上げ

製作は完了し、冷却試験中＠KEK

- ヘリウム3の代わりにヘリウム4を使用
- これまでのところ設計通りの性能を確認
  - 到達温度1.25 K　(pumping speed: 2,000 m^3/hour)
- 超流動リークなし
- 今後ヒーターによる熱負荷試験

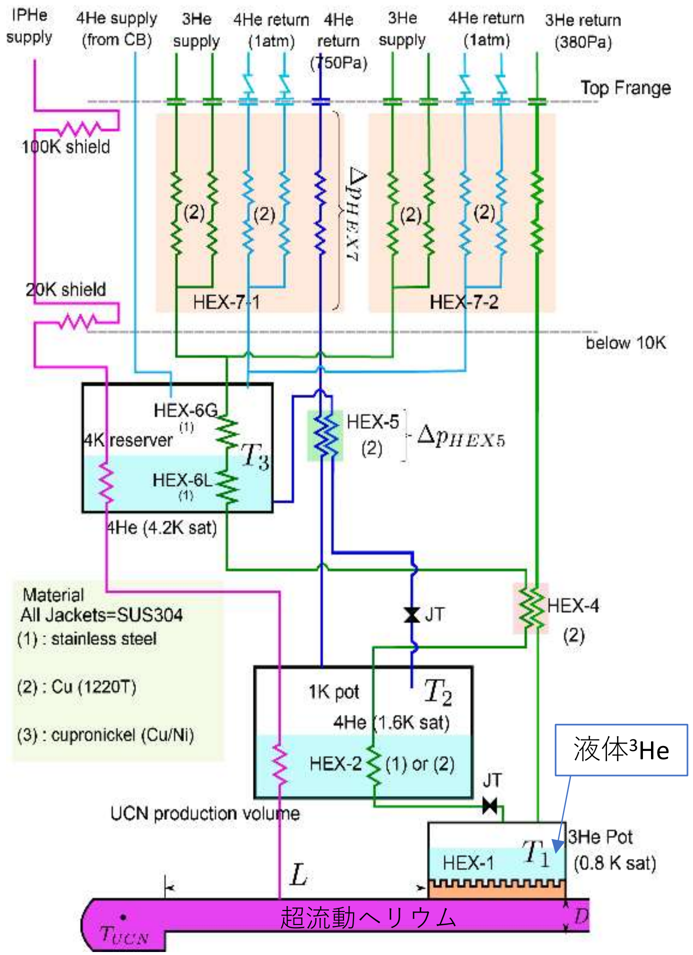

フローダイアグラム

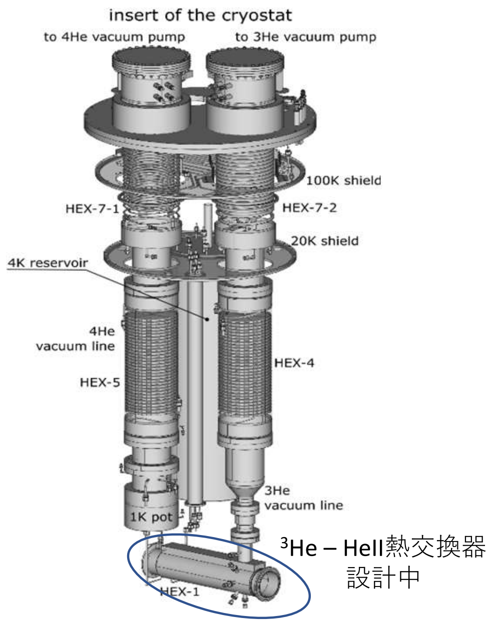

2. Kapitza Conductance

- Kapitza conductance is Conductance at the surface between liquid and solid is small at low temperature
- Kapitza conductance, $h_K(T)$ is a function of temperature.
- There are several theory on Kapitza conductance.
  - Phonon limit
    - $h_K(T)$ ~ $4500\ T^3$ [W/m^{2}K]
      - 2 - 10 times larger than measured
  - Khalatnikov theory
    - $h_K(T)$ ~ $20\ T^3$ [W/m^{2}K]
      - 10 - 100 times smaller than measured
- Experimental data strongly depends on surface quality

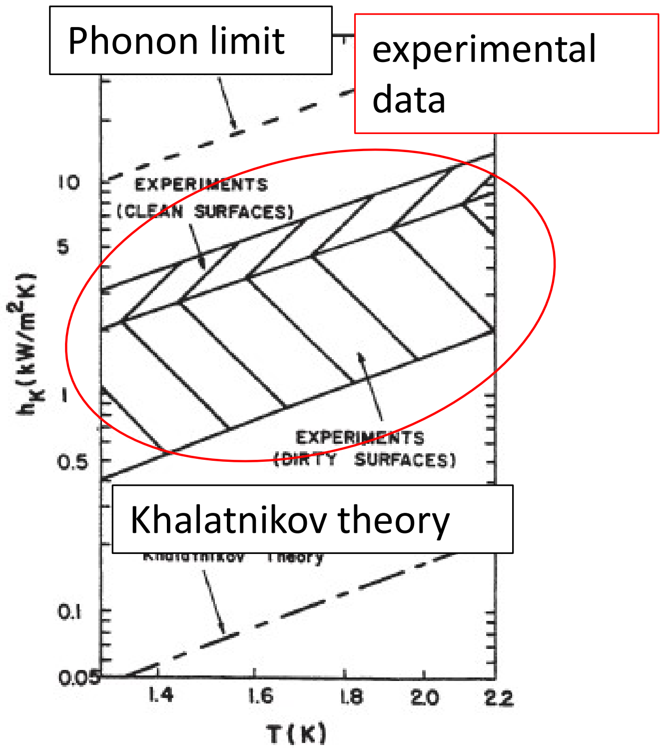

Kapitza conductance
between Copper and He-II
Helium cryogenics, Steven W. Van Sciver

Heat exchanger

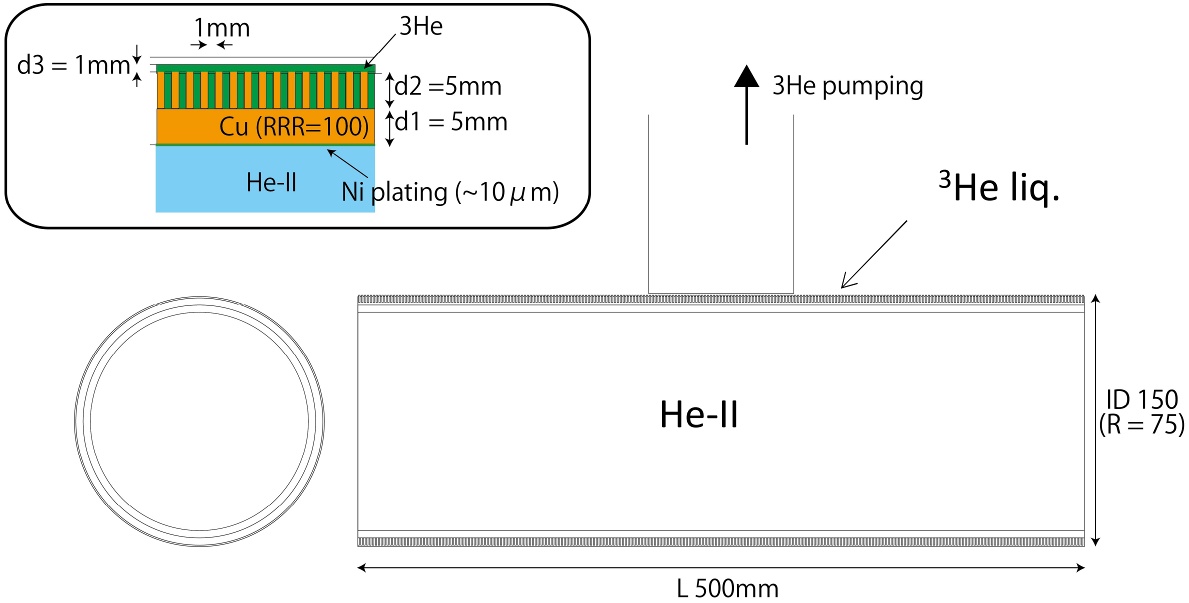

Cu Heat exchanger should be plated by Ni

Kapitza conductance between Cu-Ni is large enough since junction is solid-solid

- Kapitza conductance between Ni and He-II

  $h_{K\ Ni}$ (T) = f*h_K_{K_Cu}(T)   f = 0.61
- Kapitza conductance between Cu and 3He

  h_K(HeII) = (1.2 – 2.6) h_K(3He)

ex) K_G = 40 , T_{3He} = 0.8 K, Q = 11 W
- junction between 3He and Cu
  - $\Delta T_{Cu\text{-}3He}$ = 0.078 K
  - T_{Cu} = 0.878 K
- junction between Cu and He-II
  - ΔTNi-HeII = 0.118
  - $T_{He\text{-}II}$ = 0.996 K

Temperature difference in the heat exchanger can be neglected

Kapitza conductance Measurement

Kapitza conductance test at KEK

- Sample
  Material : OFHC
- Temperature range : 1.82 - 2.15 K

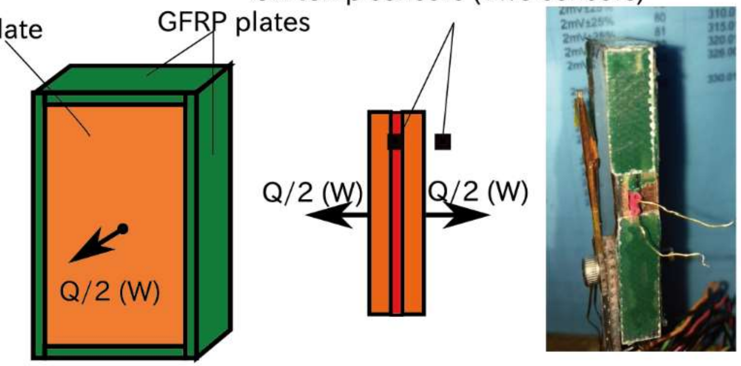

Test sample

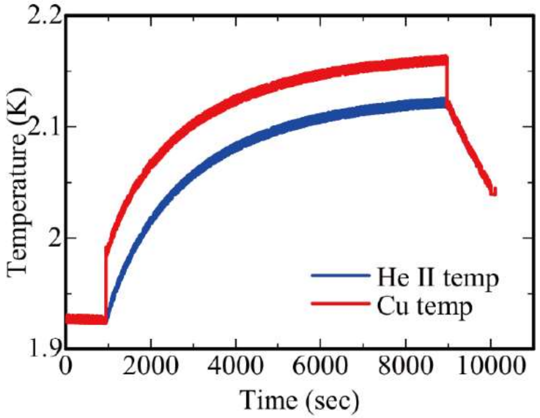

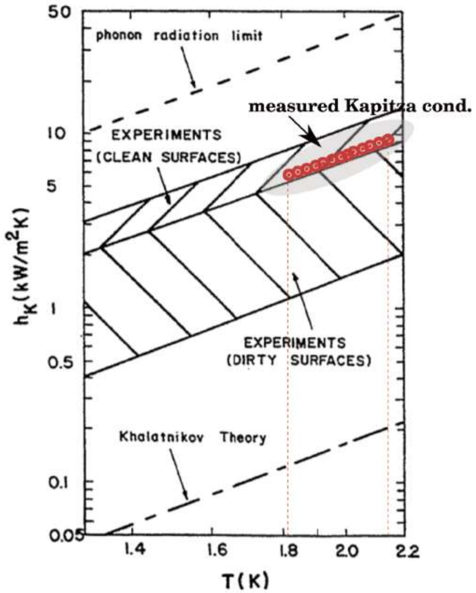

Van Sciver, Helium cryogenics

<u>Result</u>

- Dependence of T^3
- Enough Kapitza conductance

フィン形状でも同様の結果が得られるかテスト中

HEX1 prototype test

- 1/10 length model
- fin
  - 1mm width
  - 1mm gap
  - 2mm height
- installed to helium cryostat
- Cool down test
  - using 4He
  - test on going

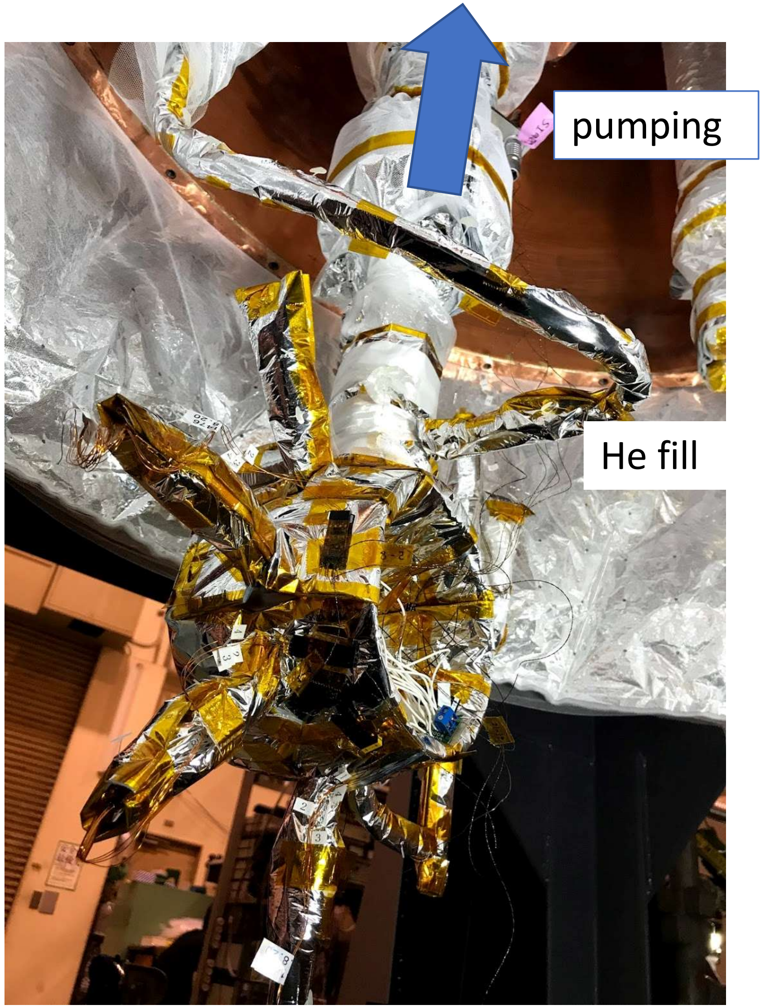

3. Superfluid Helium Heat transport

Two Fluid Model

	Normal fluid	Superfluid
Viscosity	H_n	$\eta_s = 0$
Entropy	S_n	$S_s = 0$

- Ratio of super/normal component depends on temperature dependence.
- fraction of normal mode become small in low temperature.

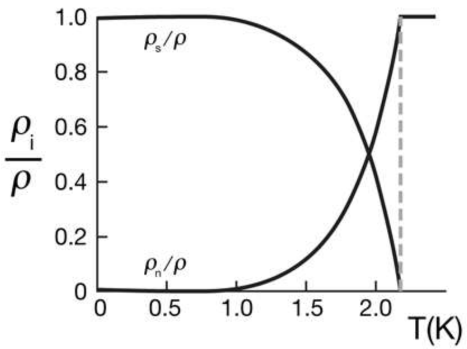

10.1103/Physics.3.5

Heat transport

- Since superfluid has no entropy, heat is transported only by normal fluid.
- Heat transport in low temperature (< 1K) become small because of small fraction of normal fluid

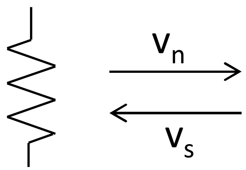

Gorter-Mellink equation

$$Q_{in} = \left(\frac{A^3}{L} \int_{T_L}^{T_H} f(T)^{-1} dT \right)^{1/3}$$

T_L : He-II temperature at the heat exchanger
T_H : He-II temperature at the UCN production volume
A : cross section of He-II
diameter = 150 mm
L : distance of heat transfer (L = 2.0 m)

f(T) : Heat transfer function

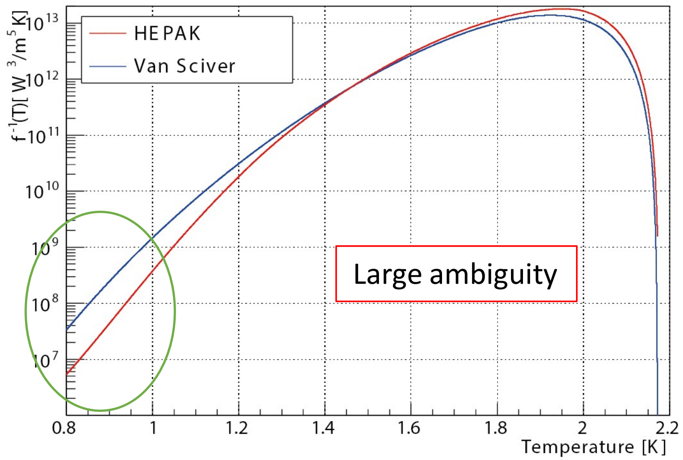

極低温で著しい熱コンダクタンスが低下 -> 1K 以下の実験値がないため実測計画中

Temperature distribution in our system

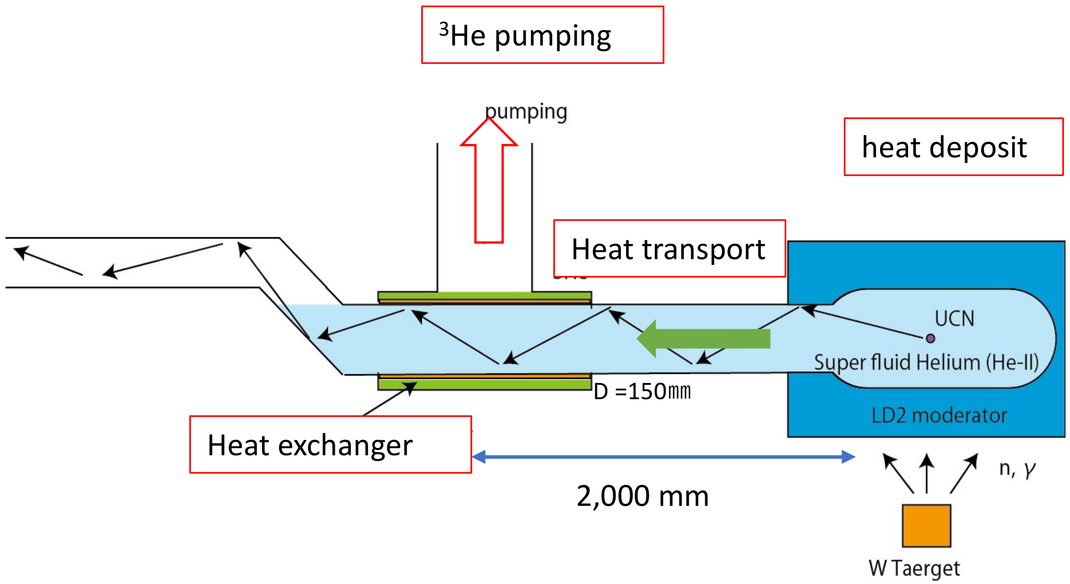

$$T_{prod} = T_{3He} + \Delta T_{3He\text{-}Ni} + \Delta T_{Ni\text{-}HeII} + \Delta T_{HeII}$$

^{3}He pumping

Kapitza cond.

Heat transfer in He-II

Temperature distribution

- ^{3}He pot

  T_{3He} = 0.800 K

Kapitza cond.
(KG = 40)

- Heat exchanger

  T_{HEX} = 0.878 K

- He-II at HEX

  $T_{He\text{-}II1}$ = 0.996 K

GM heat transfer

- He-II at UCN prod.

  $T_{He\text{-}II}$ = 1.14 K (HEPAK)
  = 1.10 K (Van Sciver)

Current design meets our requirement
Temperature at the production volume < 1.15 K

予想統計感度

UCN生成率	2.6×10^{7} UCN/sec
UCN密度 @ UCN源	6,400 UCN/cm^3
UCN密度 @ nEDM測定領域	250 Pol. UCN/cm^3

- UCN源アップグレード
  - LD2モデレーター
  - 新ヘリウム冷凍機による20kWオペレーション
- UCNトランスポート効率 : 4 %
  - MCシミュレーションによる見積もり

統計精度

$$\sigma_d = \frac{\hbar}{2\alpha E t_c \sqrt{N}}$$

E = 10kV/cm
t_c = 130s
α = 0.8 (visibility)

N : UCN数
セルサイズ ϕ 36 cm × H 15 cm (15L)×ダブルセル
N = 7.8×10^{6} UCN/batch

$\sigma_d = 1 \times 10^{-27}$ ecmの統計精度に達するまでに必要な日数

400 日

(1 cycle : 8 fill to determine the resonant frequency)

assume stable running of 14 hours/day

nEDM 測定装置

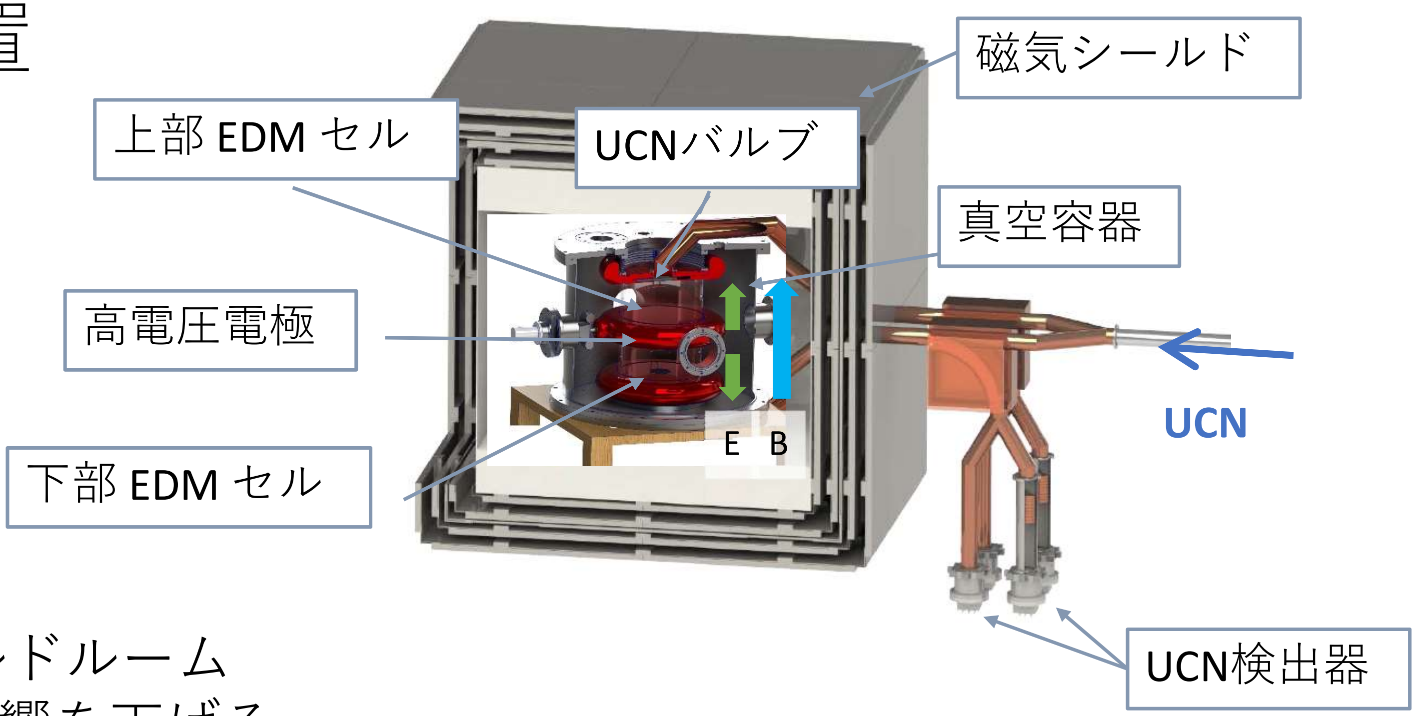

- 4重磁気シールドルーム
  外場の影響を下げる
- 上下 EDM セル
  磁場の変動を相殺する
- 自己遮蔽型コイル
  磁場の一様性の向上
- 共存磁束計
  磁場の変化を監視する

系統誤差： 10^{-27} ecm

Timeline

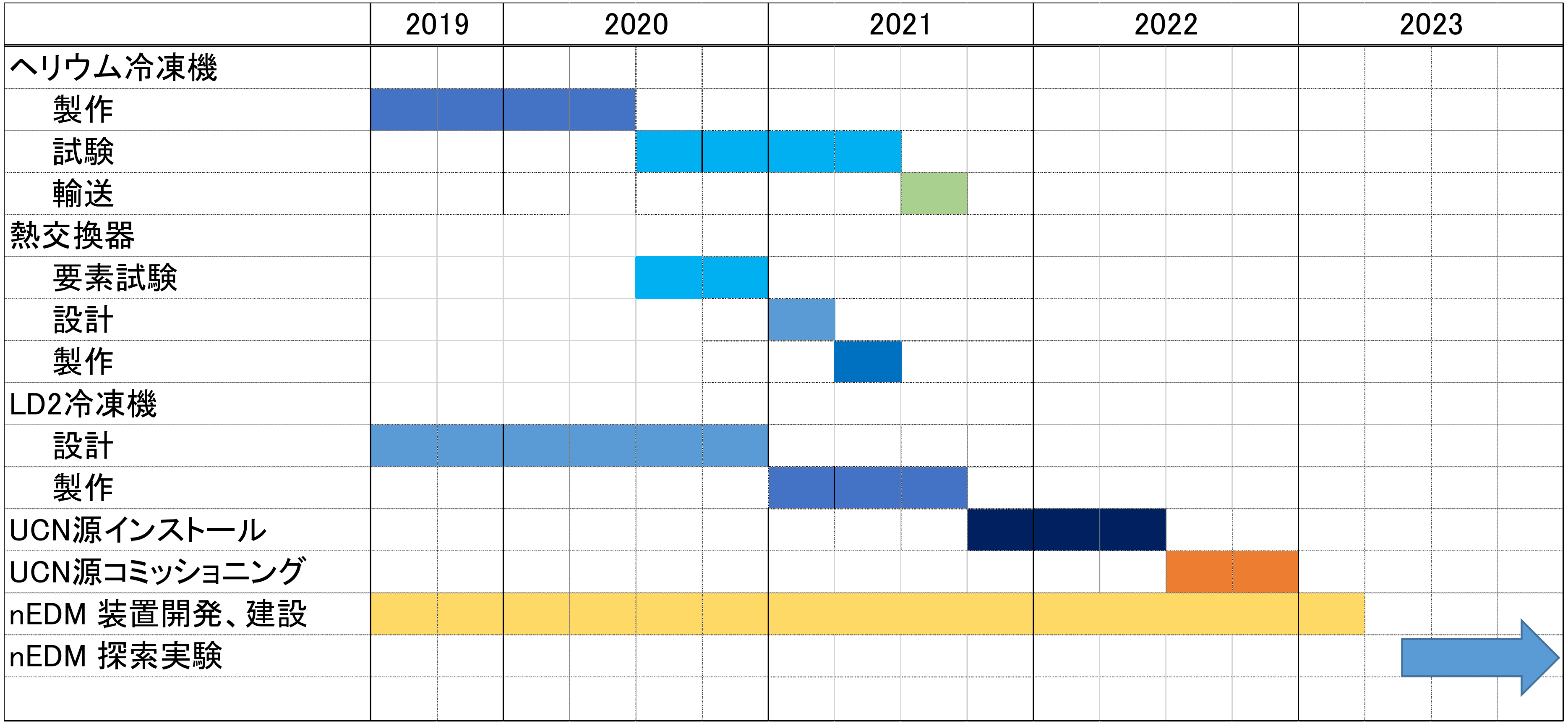
2019
2020
2021
2022
2023
ヘリウム冷凍機
製作
試験
輸送
熱交換器
要素試験
設計
製作
LD2冷凍機
設計
製作
UCN源インストール
UCN源コミッショニング
nEDM 装置開発、建設
nEDM 探索実験

Summary

- 有限の値のEDMの存在 → T対称性の破れ
  (CPT対称を仮定すれば) CP対称性の破れ
- 様々な系でEDMの測定がされているが、いまだに有限の値は見つかっていない
- 中性子EDM探索実験
  - 現在のupper limit $|d_{\mathrm{n}}| < 1.8 \times 10^{-2}$ ecm (PSI, 2020)
  - 10^{-27} ecm の感度を目標とした次期計画
    - n2EDM @ PSI
    - TUCAN
  - 高強度UCN源開発
    - UCN:物質容器に閉じ込め可能な面白い中性子
    - 超流動ヘリウムを用いたUCN源@TRIUMF (TUCAN)

回転座標系のベクトルの時間変化

S系：実験室系

S’系: S系に対し、角速度$\boldsymbol{\omega}$で回転している座標系

$$\left.\frac{d\boldsymbol{A}}{dt}\right|_{S} = \left.\frac{d\boldsymbol{A}}{dt}\right|_{S'} + \boldsymbol{\omega} \times \boldsymbol{A}$$

Inertial frame (S)

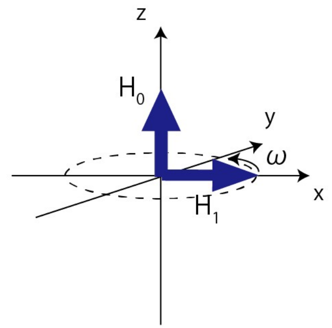

磁気モーメント***M***の時間変化

S系

$$\left.\frac{d\boldsymbol{M}}{dt}\right|_{S} = \boldsymbol{\gamma}\,\boldsymbol{M} \times H$$

S’系

$$\left.\frac{d\boldsymbol{M}}{dt}\right|_{S'} = \left.\frac{d\boldsymbol{M}}{dt}\right|_{S} - \boldsymbol{\omega} \times M$$
$$= \boldsymbol{\gamma}\mathbf{M} \times (\boldsymbol{H} + \frac{\boldsymbol{\omega}}{\boldsymbol{\gamma}})$$

rotating system (S’)

rotating speed : ω

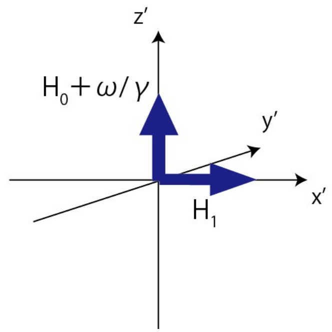

z方向に静磁場H_0、xy平面に回転磁場H_1がかかっているとき、

$$\omega_0 = \gamma H_0 \quad \text{(resonant frequency)}$$

の時、S’系ではH = (0,H1,0)となり、スピンンはy’z’平面上を回転する

Prototype UCN Source

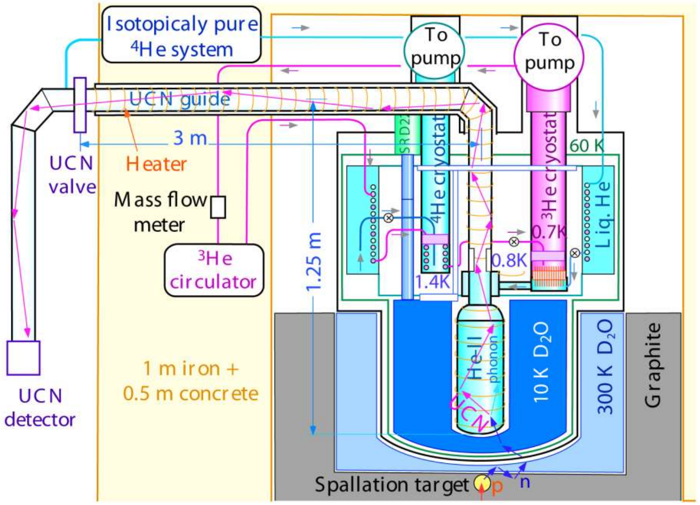

Previous UCN source

He-II bottle

Φ16cm , L 41cm, Volume = 8L

Al of 2mm thickness, inner wall coated with nickel

Surrounded by D_2O moderator (ice, water)

Cryostat

keep He-II the temperature by ^{3}He pumping

^{3}He is pre-cooled by ^{4}He pumping

UCN guide

Φ8.5 cm, L = 3 m

1.25m high from He-II bottle

Improvement of UCN Storage time

Year	τ_s	T_{HeII}	Improvement
2002	14 s	1.2K	
Jun 2006	29 s	0.9K	Use ^{3}He cryostat
Nov 2006	34 s	0.8K	Reduce HeII film perimeter (8.5 cm → 5 cm)
Jul 2007	39 s	0.8K	Remove ^{3}He contamination
Apr 2008	47 s	0.8K	Fomblin coating
Dec 2009	61s	0.8K	Alkali cleaning
Feb 2011	81s	0.8K	High temperature baking (140℃)

remove He contamination is important

UCN Production by the Prototype source

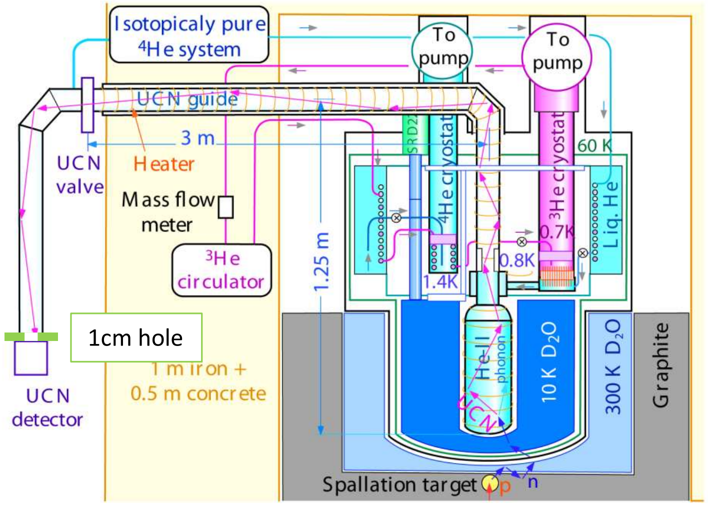

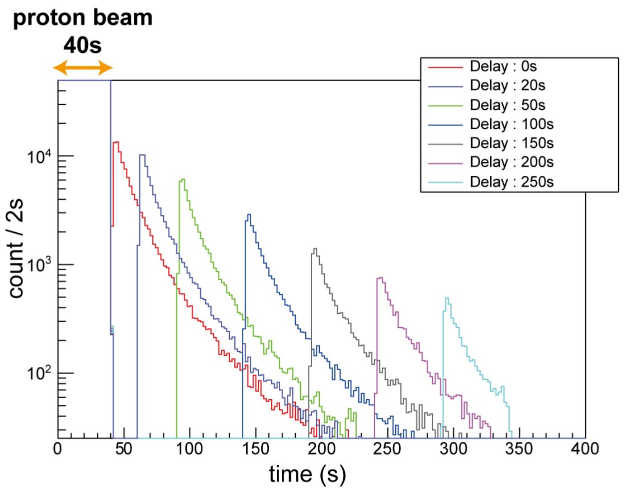

Storage life time measurement
Counting UCN after valve opening

UCN is produced and hold in the UCN bottle and guide
After time delay UCN valve open

Storage Lifetime : **81 sec**
UCN density
26UCN/cm^3 Ec = 90 neV
400 MeV × 1 μA = 0.4 kW
Y, Masuda et. al., Phys. Rev. Lett. 108, (2012), 134801

UCN source in the world

	Source Type		UCN density [UCN/cm^3] $\rho \propto Ec^{3/2}$	Max energy Ec [neV]	Lifetime [s]
	neutron	Moderator			
Ours @ RCNP/TRIUMF	Spallation	He-II	26@1μA	90	150
Ours @ future	Spallation	He-II	1300 pol	90	150
Sussex-RAL-ILL	Beam	He-II	1000	250	150
SNS	Beam	He-II	150	134	500
PNPI	Reactor	He-II	12000	250	23
Los Alamos	Spallation	SD_2	200	180	1.6
PSI	Spallation	SD_2	1000	250	6
Munich	Reactor	SD_2	1000 pol	250	**

There are a lot of UCN facility (including plan)

HEX1 development

- HEX1 prototype1
  - annular fins
    - push up liquid ?
- HEX1 prototype 2
  - vertical fins
    - fin pitch optimization is necessary
- HEX1 prototype 3
  - full size model
  - not final design
  - fin: annular or vertical or no fin
    - less 3He model
  - will be installed first cooling at TRIUMF
    UCN production?

  - Final model will be installed later

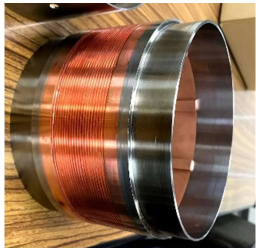

prototype 1

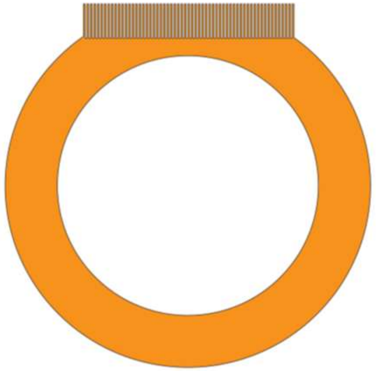

prototype 2

GRANIT

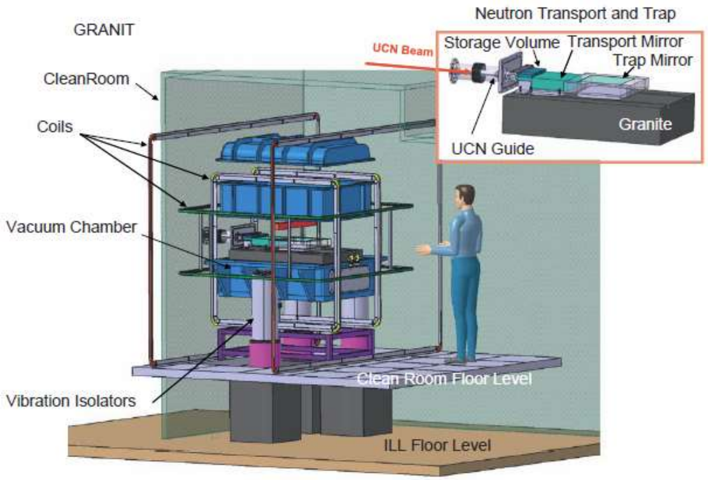

Fig. 1. GRANIT spectrometer.

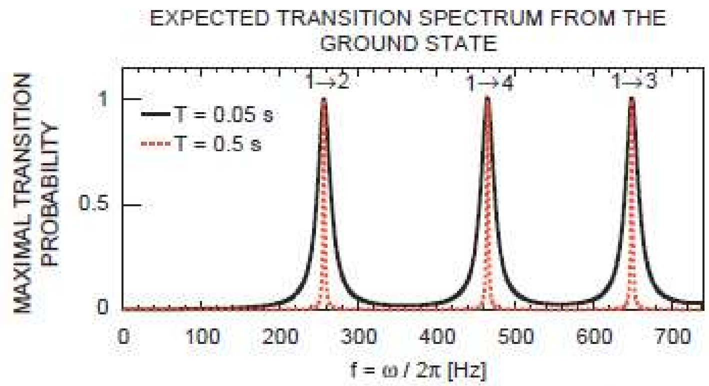

Fig. 3. Maximum probability for a neutron to leave the ground state is shown as a function of the excitation frequency for two different excitation times.

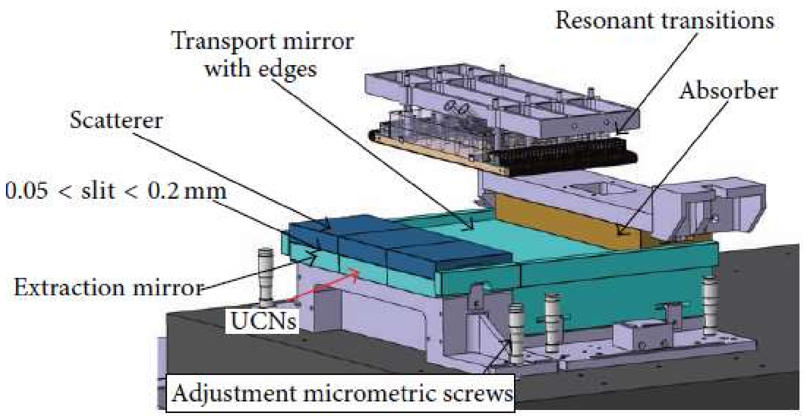

magnetically induced resonance transition

- extraction mirror and scatter
  - select low vertical velocity component
- transport mirror
  - a periodic magnetic field induce resonant transition between quantum states
- absorber
  - filter quantum state

M. Kreuz et al. NIM A 611 (2009) 326–330
D. Roulier et al. Advances in High Energy Physics Volume 2015, Article ID 730437,

Neutron detector

Since neutron has no charge, it is not possible to detect directly by the electrical signal

- Use nuclear reaction (neutron converter)
  - ^{3}He (σ = 5333 barn)
    - $^{3}He + n \rightarrow {}^{3}H + p + 0.765$ MeV   Gas detector
  - ^{6}Li (σ = 940 barn)
    - $^{6}Li + n \rightarrow \alpha + {}^{3}H + 4.78$ MeV
  - ^{10}B (σ = 3835 barn)   Scintillator etc.
    - $^{10}B + n \rightarrow \alpha + {}^{7}Li + \gamma + 2.79$ MeV   93.9%
    - $^{10}B + n \rightarrow \alpha + {}^{7}Li + 2.79$ MeV   6.1%

2 Dimensional UCN Detector

S. Kawasaki et.al. , NIM A 615 (2010) 42–47

- ＣＣＤ sensor

HAMAMATSU S71710-0909

Active Area	12.288 × 12.288 mm^2
Number of Pixels	512 × 512
Pixel Size	24 × 24 μm^2
Full Well Capacity (Vertical)	300 ke$^-$
Full Well Capacity (Horizontal)	600 ke$^-$
Dark Current Max. 0°C	600 e$^-$/pixel/s
Readout Noise	8 e$^-$ rms

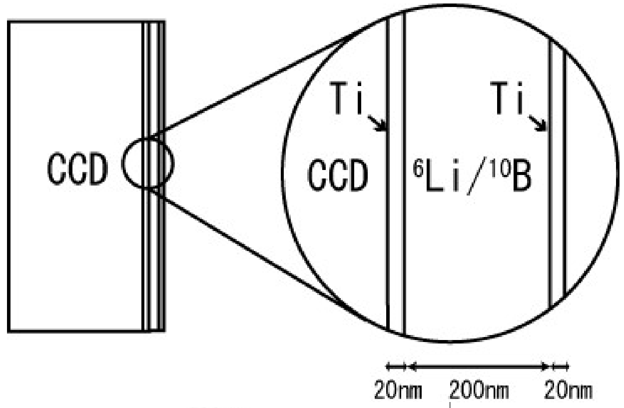

neutron converter

$$n+{}^{10}B \rightarrow \alpha(1.47\mathrm{MeV})+{}^{7}Li(0.84\mathrm{MeV})+\gamma(0.48\mathrm{MeV}) \quad 93.9\%$$
$$\rightarrow \alpha(1.78\mathrm{MeV})+{}^{7}Li(1.01\mathrm{MeV}) \quad 6.1\%$$
$$n+{}^{6}Li \rightarrow \alpha(2.05\mathrm{MeV})+{}^{3}H(2.73\mathrm{MeV})$$

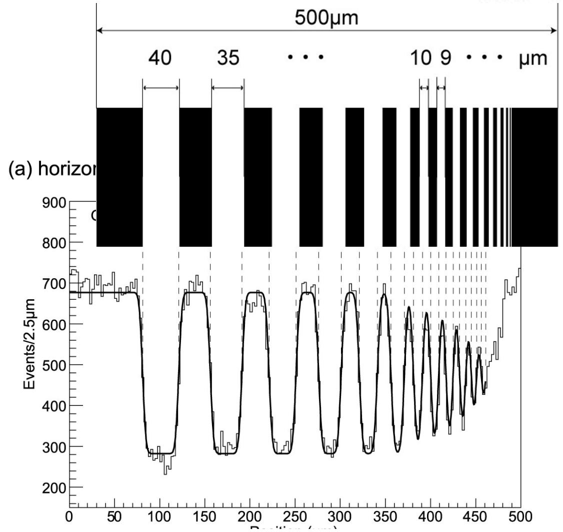

Gd absorber

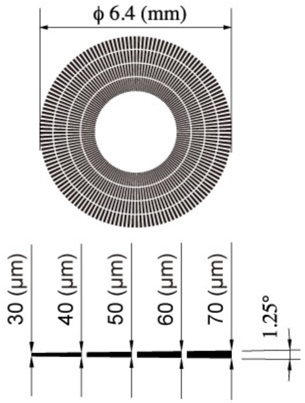

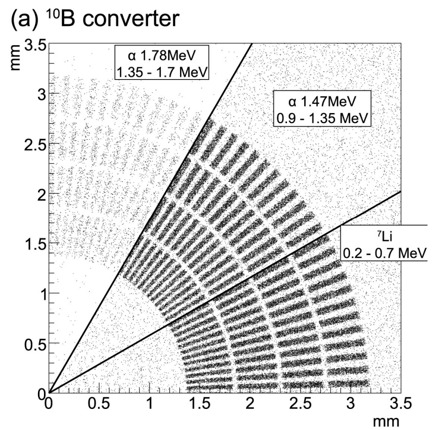

spatial resolution
2.9 ± 0.1 μm

Fine-grained nuclear emulsion

High spatial resolution 3D tracking detector

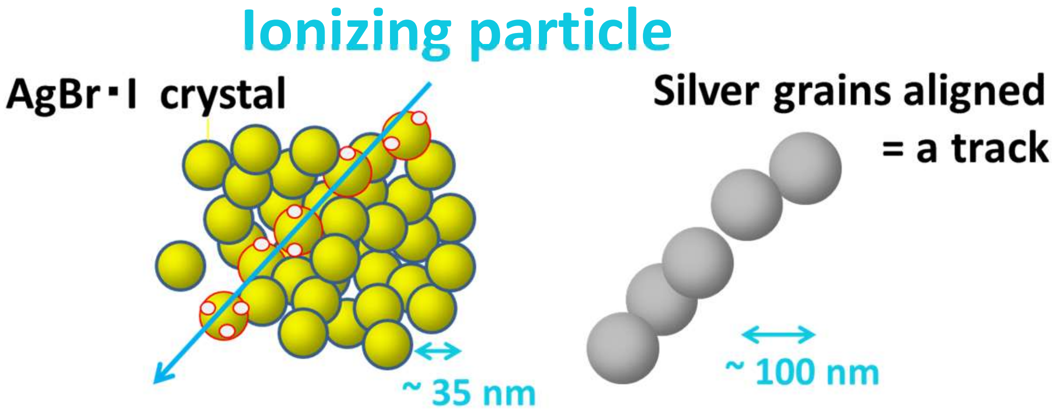

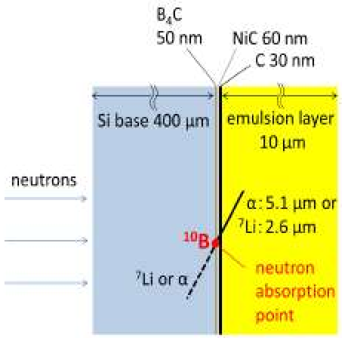

Figure 3. A cross sectional view of the thin layer (B_4C) type detector. An α particle and a ^7Li are emitted back-to-back from neutron absorption by ^{10}B. One of them will be detected inside the emulsion layer. The absorption point will be determined by extrapolating the track to the B_4C layer.

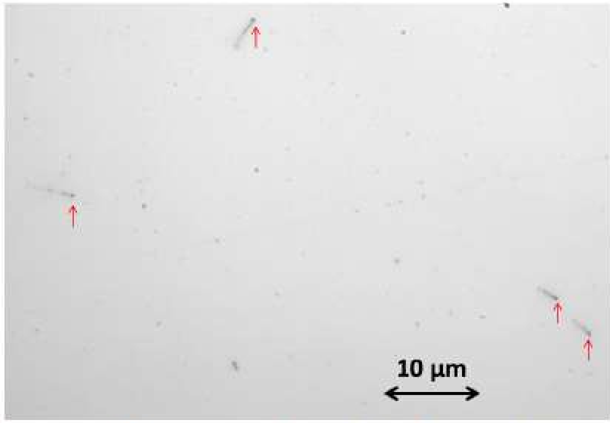

Figure 4. A microscopic view of four tracks of α particles or ^7Li s emitted from neutron absorptions by ^{10}B. Arrows show the starting points of the tracks.

Neutron converter

+

3D tracking of emulsion

||

submicron spatial resolution

N. Naganawa et al. POS (KMI2017) 077

Crystal EDM

- 結晶内を透過する冷中性子のスピン位相の変化を観測
- 結晶内の大きな有効電場を用いることによって感度をあげる
- 有効電場・体積の大きな結晶を用いるのが鍵

- Current best value
  dn = (2.5 ± 6.5stat ± 5.5sys) × 10^{-24} ecm at ILL
  V.V. Fedorov et al Phys. Lett. B 694, 22 − 25 (2010)
- 精度を上げた実験がJ-PARCやESSで計画されている

Sensitivity of nEDM experiment $\sigma(d_n) \propto \frac{1}{E\tau\sqrt{N}}$

E : strength of applied electric field
τ : interaction time
N : neutron counts

	Free flight metod	Crystal diffraction method	UCN method
interaction tome τ [s]	$\sim 10^{-1}$	$\sim 10^{-3}$	$\sim 10^{2}$
electric field E [V/cm]	$\sim 10^{4}$	$\sim 10^{8}$	$\sim 10^{4}$
neutron counts n [n/s]	$\sim 10^{8}$	$\sim 10^{4}$	$\sim 10^{2}$
sensitivity σ(d_n)	$\sim 10^{-25}/\sqrt{\mathrm{Day}}$	$\sim 10^{-25}/\sqrt{\mathrm{Day}}$	$\sim 10^{-25}/\sqrt{\mathrm{Day}}$

伊藤さん(名古屋大)のスライド

パルス中性子源を用いた結晶回折によるnEDM探索

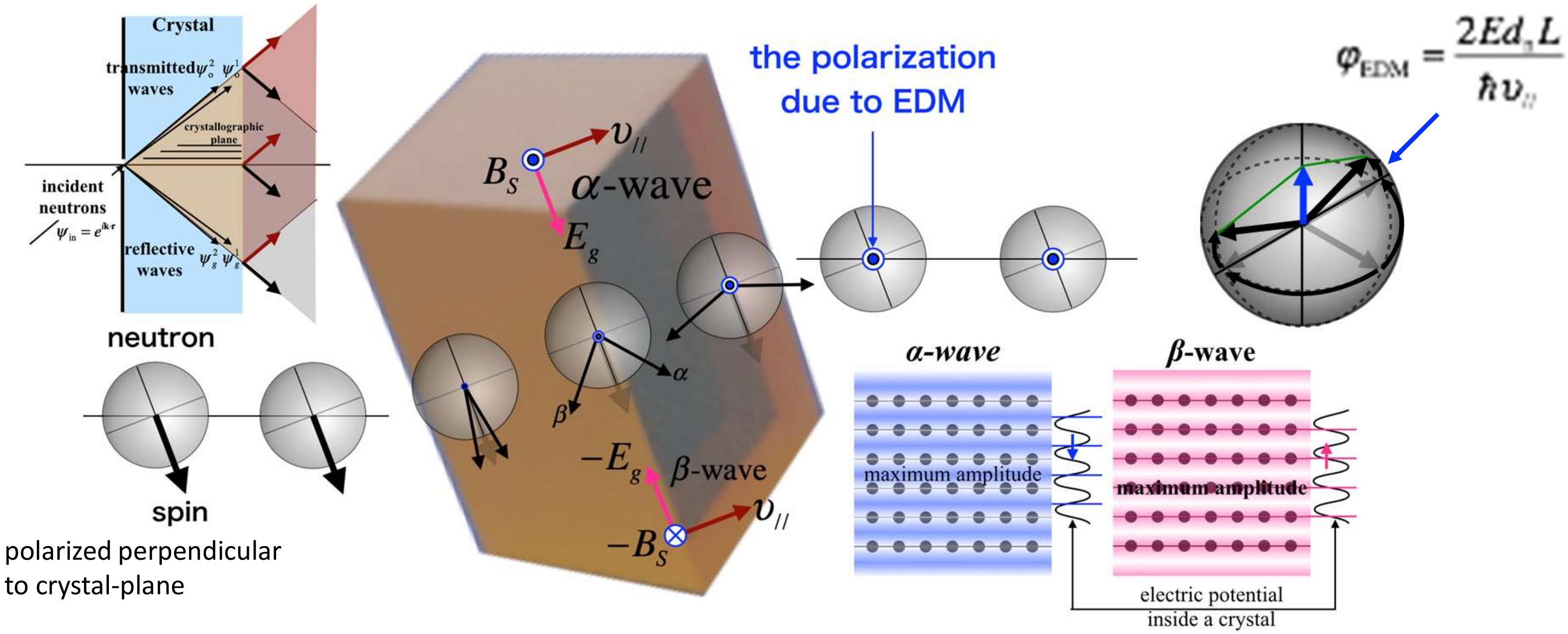

ペンデル縞を用いた結晶内電場の測定

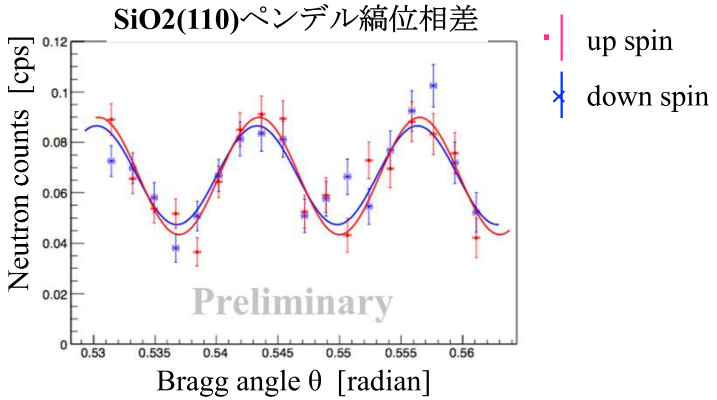

$$E_g = (0.40 \pm 1.47) \times 10^8 \ [\mathrm{V/cm}]$$

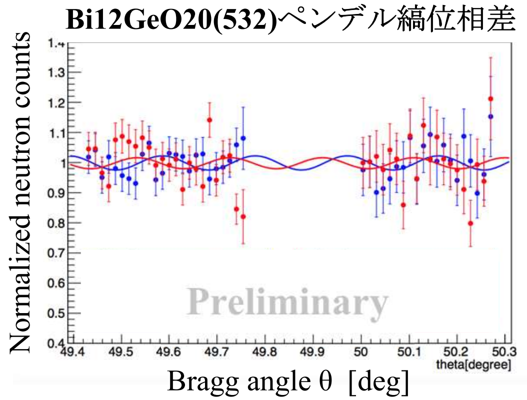

$$E_g = (3.5 \pm 2.0) \times 10^8 \ [\mathrm{V/cm}]$$